มหาวิทยาลัยมหิดล
Mahidol University

1-D Vertical Electrical Sounding (VES) Inversion with a lateral constraint

Submitted June 2020, in partial fulfillment of the conditions

For the award of the degree **Bachelor of Science in Physics.**

Panyawat Suriyapor

Advisors

Dr. Puwis Amatyakul

Geophysics Research Group, Department of Physics

Faculty of Science, Mahidol University

June, 2020

Abstract

Vertical Electrical Sounding (VES) method is an electrical method of geophysics prospecting that widely used to image the shallow subsurface resistivity structure with a typical depth of investigation less than 1 km. The injecting current and the measured voltage acquired via electrode arrays will be transferred to apparent resistivity as the data of the investigation to obtain the 1D resistivity beneath the investigation area. For the investigation area where several VES stations are conducted, the 1D resistivity inversion is usually performed individually for each station. However, the obtained 1D resistivity model can totally differs for the nearby station due to limitation of the 1D inversion.

This research interest is therefore to integrate the nearby VES sites into the inversion with the assumption that the geological structure would not have the rough change. I have developed the 1-D VES inversion code base on Occam's inversion with adding the lateral constraint into the objective function of the optimization. The lateral constraint can be considered by modifying the roughness operator to also incorporate the nearby resistivity model of other VES sites. The system of the inversion is also modified to gather all the data and model parameters of the VES sites simultaneously. The developed code was also applied with the real data from geophysics exploration at Sai Yok, Kanchanaburi, Thailand. The result shows that the developed VES inversion code can calculate the 1-D resistivity model of the acquired data from the study area.

Keyword: Vertical electric sounding, VES, Geophysical prospecting, 1D modelling, Lateral constraint.

Acknowledgment

In this project, I would like to especially thank my advisor “Dr. Puwis Amatyakul” for kind supporting and advice in both works and daily life. Moreover, I would like to express my special thanks gratitude for more information and the warm welcome from all of the people in Geophysics research group at Mahidol University. Finally, I would like to thank Faculty of Science Alumni Association, Mahidol University scholarship for funding support.

Contents

List of Figures

Chapter 1

Introduction

In the present, humans use natural resources which were obtained from underground in daily life until industrial. The investigations and excavation cost and time for finding underground natural resources are dramatically increased following the deepness, according to the reason, the scientific suggestion is very important in order to assure the location of resources, decrease cost and time. The vertical electric sounding (VES) is one of the electrical methods for estimating the resistivity model of the subsurface structure by using the unique property of the object that effects to the electrical current streamline in the different the medium and measured voltage due to subsurface resistivity distribution, electrode spacing and measured voltage on the surface can be used to speculate the resistivity model by the inversion method. The forward modeling is the process that transforms the resistivity model to voltage and current on the surface which is a crucial part of the inversion process, consequently, the result from the inversion can be used as suggestions for various resources explorations.

1.1 Motivation

The research in the vertical electrical sounding survey (VES) is important for shallow geophysical explorations. 1D VES inversion was used for generating the subsurface 1D resistivity model from acquired data from VES exploration stations. The subsurface resistivity model from the inversion system was interpreted to use in other activities such as drilling or building which all of that high cost. But the inversion system is a nonlinear problem that means same acquired data can generate many subsurface resistivity models which can totally different, so, after generating and interpreting the models, the user has to select one of the obtained models from the calculation which is possible and dependable with the survey location to be the model for using. From the reason above the interpretation of obtained models have to use other data such as data of geological exploration or obtained models from nearby stations in interpretation together. For the investigation area where several VES stations are conducted, the 1-D resistivity inversion is usually performed individually for each station that makes this method is difficult and taking a long time for selecting and comparing. Leading to the motivation of this project, if the user can generate the subsurface resistivity models by joint the acquired data from nearby stations in the calculation part, the obtained subsurface resistivity models will be related together that help to reduce the selecting and comparing models time.

1.2 Aims and Objectives

This research aims at a development important component of the inversion process by adding the lateral constraint into the inversion process and generate a 1D VES inversion code with lateral constraint. The result of this research is the 1D Vertical Electrical Sounding (VES) inversion program which was added the lateral constraint. This inversion program is expected to be useful in both industrial and academic purposes.

1.3 Inverse and Forward Problem

The relation between the model and measured data in a perfect experiment is represented by the following equation.

$$F(m) = d$$

where F is forward modeling operator, m is the model and d is the data. The forward problem is to find d from given m and the inverse problem is to find m from given d. The inversion process also has forward modeling as a very important part, therefore, despite the inversion process is the uppermost objective, forward modeling is an objective that cannot be neglected as shown by figure 1.1.

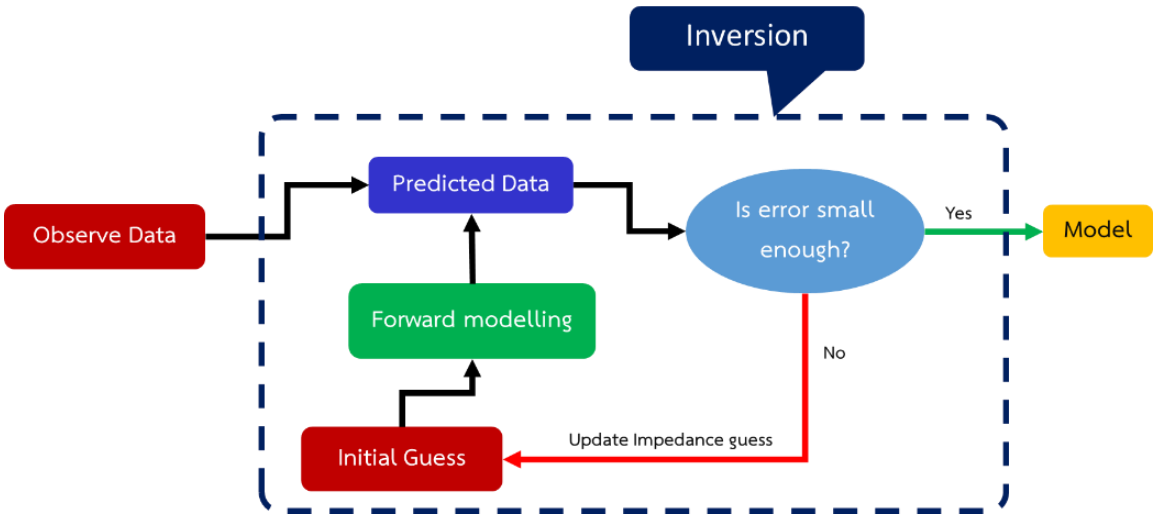

Figure 1.1 : Inversion process

1.4 Electrical Survey

Electrical geophysical prospecting methods detect the surface effects produced by electric current flow in the ground. Using electrical methods, one may measure potentials, currents, and electromagnetic fields that occur naturally or are introduced artificially in the ground. In addition, the measurements can be made in a variety of ways to determine a variety of results. There is a much greater variety of electrical and electromagnetic techniques available than in the other prospecting methods, where only a single field of force or anomalous property is used. Basically, however, it is the enormous variation in electrical resistivity found in different rocks and minerals that makes these techniques possible

1.4.1 Vertical Electrical Sounding (VES)

The VES method is a geophysical electrical survey technique used to probe the Earth. It is one of the popular surveying methods for imaging the shallow subsurface resistivity structure because of its convenience and its low environmental impact compared to other methods. The source of the VES method is direct current. When a direct current (I) is injected into the ground of the area of interest, the potential value (V) is measured. Then, the measured data are used to calculate the apparent resistivity, which is obtained by assuming that the subsurface is homogenous. From Ohm's law which states that the resistance in the area of interest is V/I, we can obtain the resistance (R). Then, we multiply the obtained resistivity by a factor called the "geometric factor" to find the apparent resistivity. The geometric factor depends on the chosen type of electrode array.

1.4.1.1 Electrodes Array

The electrodes array is the arrangement of the electrodes in the profile and generally consists of four electrodes. There are three favorite electrode arrays, namely the Wenner, Dipole-Dipole, and Schlumberger array. Each electrode array senses the underground structure difficultly. Therefore choosing the electrode array will depend on the interesting features underground.

1.4.1.1.1 Wenner Array

The Wenner array is the electrode array used to study the subsurface structure in which vertical difference. Generally, the electrodes of the Wenner array will be arranged as shown in Figure 1.2. The characteristic of the Wenner array is the equally-separated distance (na) between each electrode.

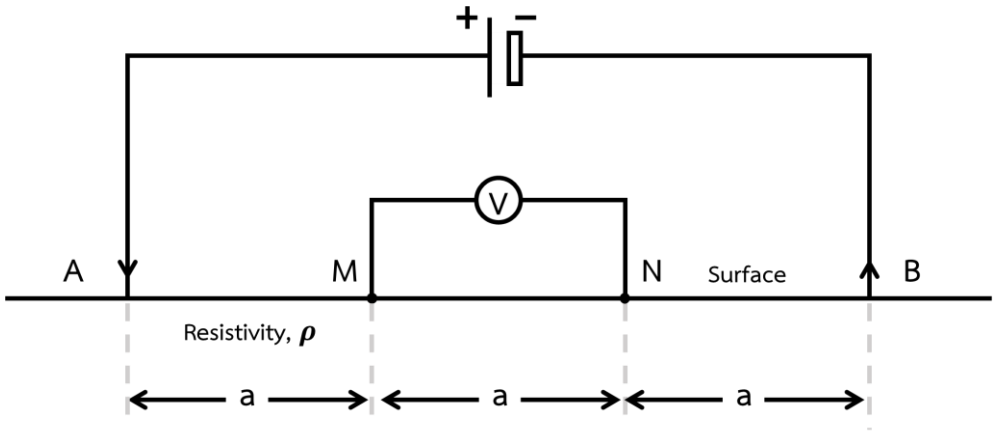

Figure 1.2 : Wenner array

The apparent resistivity can be determined from

$$\rho_a = 2\pi n a \frac{V_{MN}}{I}$$

where the $2\pi na$ is the geometric factor of the Wenner array, n is an integer and V_{MN} is the potential difference between electrode M and N. The procedure of obtaining the geometric factor is starting from Ohm's law,

$$E = \rho J = \rho \frac{I}{4\pi r^2}\hat{r}$$

where ρ is resistivity or inverse of conductivity σ, r is the distance from the source to the point of interest, E is the electric field and J is the current density. When the current is injected into the homogeneous earth, the electric field will differ in hemispherical shape into the earth. Thus, can be rewritten in the form of potential as,

$$V(r) = \int_r^\infty E\, dr = \int_r^\infty \frac{\rho I}{2\pi r^2}\, dr$$

Solving equation above, the potential is obtained in the form of

$$V(r) = \frac{\rho I}{2\pi r}$$

We can find the potential at any the electrode point by combining the potential generated from A and B which is equal to

$$V_p = \frac{\rho I}{2\pi}\left(\frac{1}{AP} - \frac{1}{PB}\right)$$

where AP is the distance between electrode A and point P, PB is the distance between electrode B and point P. So, the potential difference between electrode M and N is then equal to

$$\mathrm{V_{MN}} = \mathrm{V_M} - \mathrm{V_N} = \frac{\mathrm{I}\rho}{2\pi}\left[\left(\frac{1}{\mathrm{AM}} - \frac{1}{\mathrm{MB}}\right) - \left(\frac{1}{\mathrm{AN}} - \frac{1}{\mathrm{NB}}\right)\right]$$

Thus we can find the resistivity from

$$\rho = \frac{\mathrm{V_{MN}}}{\mathrm{I}}\mathrm{K}$$

where

$$\mathrm{K} = 2\pi\left[\left(\frac{1}{\mathrm{AM}} - \frac{1}{\mathrm{MB}}\right) - \left(\frac{1}{\mathrm{AN}} - \frac{1}{\mathrm{NB}}\right)\right]^{-1}$$

and K is defined as the geometric factor which depends on the electrode configuration. For the Wenner array, the geometric factor is

$$\mathrm{K} = 2\pi\left[\left(\frac{1}{\mathrm{na}} - \frac{1}{2na}\right) - \left(\frac{1}{2\mathrm{na}} - \frac{1}{\mathrm{na}}\right)\right]^{-1} = 2\pi na$$

Can calculate the apparent resistivity of this array from

$$\rho_a = 2\pi na\frac{\mathrm{V_{MN}}}{\mathrm{I}}$$

We can use the same equation to calculate the apparent resistivity of the other electrode arrays, but with a difference K factor.

1.4.1.1.2 Dipole-Dipole array

The Dipole-Dipole array is used for a vast surveying area. It can be used to detect the difference in the horizontal underground structure. In general, the dipole-dipole configuration is shown in Figure 1.3.

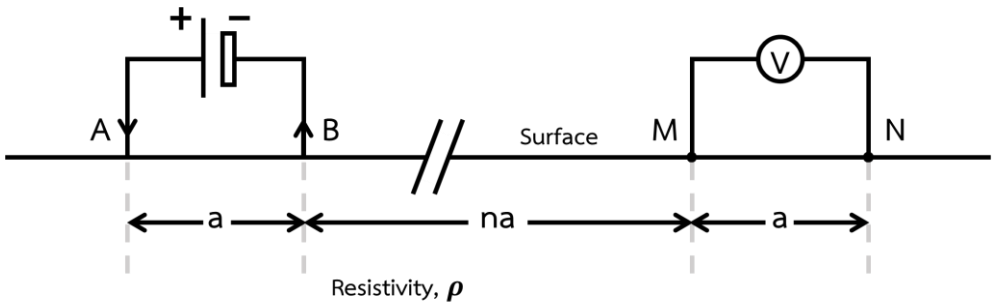

Figure 1.3 : Dipole-dipole array

The outstanding features of the Dipole-Dipole array are the sequence and range of current electrodes. Electrode A is placed close to electrode B with electrode spacing (a) which is the same as the electrode spacing between the potential electrodes M and N. If we increase the electrode spacing between B and M, we will get the apparent resistivity at greater depth. We can calculate the apparent resistivity of this array from

$$\rho_a = \frac{V_{MN}}{I} \pi a n (n+1)(n+2)$$

1.4.1.1.3 Schlumberger array

The Schlumberger array, the most popular electrode array, can detect the change of the structure in both vertical and horizontal directions. However, it is not as clear as the vertical direction in the Wenner array and horizontal direction in the Dipole-Dipole array. The Schlumberger configuration is shown in Figure 1.4.

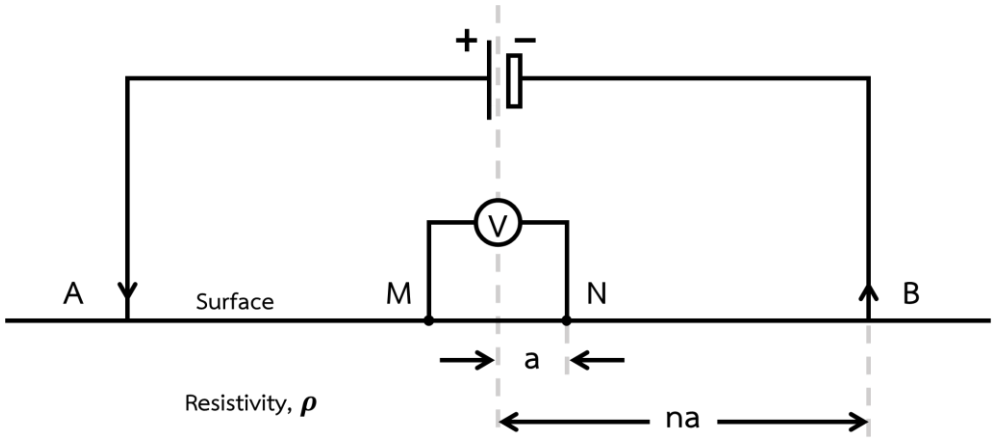

Figure 1.4 : Schlumberger array

The outstanding feature of Schlumberger is that the electrode spacing of potential electrodes M and N of the entire survey is equal to a. Moreover, if we increase the electrode spacing between electrode A and M, and electrodes B and N, it is equivalent to the apparent resistivity at great depth. The apparent resistivity of this array can be calculated from.

$$\rho_a = \frac{V_{MN}}{I}\pi\frac{b(b+a)}{a} \approx \frac{V_{MN}}{I}\pi\frac{b^2}{a}, \text{if } a \ll b$$

1.5 Chapter Summary

In this research, the development of inverse modeling of kind of one-dimension Vertical Electrical Sounding (VES) by adding the lateral constraint is the main topic. The Vertical Electrical Sounding method is famous in shallow exploration case. The potential obtained from the electrode's measurement after injection of the current into the earth is calculated to image the one-dimension subsurface resistivity model. In the calculation, the one-dimension resistivity inversion is usually performed individually for each station. But, all of the obtained one-dimension resistivity models can totally different for the nearby station because of the limitation of one-dimension inversion. So, the lateral constraint is applied to the objective function of the optimization of inverse modeling for complying with the acquired data from nearby Vertical Electrical Sounding station together to develop the obtained model. The production of this work and some further works is one-dimension Vertical Electrical Sounding inversion with lateral constraint program which is important in shallow resources exploration and study of earth structure.

Chapter 2

Background and Related Works

Forward and inverse modeling of one-dimension Vertical Electrical Sounding survey uses several relevant Mathematics and Physics concepts. This chapter will discuss these concepts, the approach for this research, to a one-dimension inversion system for co-calculation of the acquired data from nearby VES station to get model developed.

2.1 1D VES Forward modelling

Because VES forward modeling was calculated from difficult mathematic such as Bessel's function and infinite integral, it is a non-linear problem. In this project, I will focus on the inversion part, so forward modeling will be reduced into Schlumberger VES forward modeling. Schlumberger VES is different from other configurations that we assume that spacing between two measuring voltage electrodes is very small compared to the spacing between current electrodes. The main calculation in the forward modeling is resistivity transform function and its deconvolution. The deconvolution of the parameter is called "Gosh filter".

The forward modeling algorithm is an essential part of the inversion program. It is used to calculate the response (ρ_a) from the known model structure (ρ). The forward algorithm of VES can be calculated from Steafanescu's equation of electrical potential. Potential on the surface of the layered earth at distance r from a point current source I is given as

$$\rho_a(r) = r^2 \int_0^\infty T(\lambda) J_1(r\lambda) \lambda d\lambda$$

when ρ_a is apparent resistivity, J_1 is the first-order Bessel's function of the first kind, r is the half-electrode spacing or AB/2, λ is electrode parameter or 1/r, T_1 is the resistivity transform that can be calculated recursively by applied Hankel's inversion as

$$T(\lambda) = \int_0^\infty \frac{1}{r}\rho_a(r)J_1(r\lambda)d\lambda$$

For a succession of N layers, can write the resistivity transform depends only on that layer's resistivity and thickness, as well as on the value of the transform for the subjacent layer. Starting from the last layer, with $T_N = \rho_N$, it is possible to successively compute the transforms $T_{N-1}, \dots, T_2, T_1$ via the recursive relation as

$$T_i(\lambda) = \frac{\rho_i(1 - e^{-2\lambda h_j}) + T_{i+1}(1 + e^{-2\lambda h_j})}{\rho_i(1 + e^{-2\lambda h_j}) + T_{i+1}(1 - e^{-2\lambda h_j})}$$

When ρ_i is true resistivity $(\rho_1, \rho_2, \dots, \rho_N)$, h_j is thickness $(h_1, h_2, \dots, h_{N-1})$ by the last layer being considered infinitely extended.

For a two-layer section with top layer A underlain by substratum B,

$$T_{AB}(r) = \rho_A \frac{1 + k_{AB}e^{-2h_A/r}}{1 - k_{AB}e^{-2h_A/r}}$$

When $r = \frac{1}{\lambda}$ and $k = \frac{\rho_n - \rho_{n-1}}{\rho_n + \rho_{n-1}}$ so can write that $k_{AB} = \frac{\rho_B - \rho_A}{\rho_B + \rho_A}$

The resistivity transform of a section of any number of the layer can be deduced from the following iterative.

$$T_n(r) = \frac{T'_{AB} + T_{n-1}}{1 + \frac{T'_{AB}T_{n-1}}{\rho_A^2}}$$

When T'_{AB} is resistivity transform of a two layer section for special case by $k_{AB} = -1$

The application of equations above can be demonstrated by deriving an expression for T for a three-layer section ABC, where A is the top layer, B the intermediate layer and C the substratum as

$$T_{ABC}(r) = \frac{T'_{AB} + T_{BC}}{1 + \frac{T'_{AB} T_{BC}}{\rho_A^2}}$$

When $T_{BC}(r) = \rho_B \frac{1+k_{BC}e^{-2h_B/r}}{1-k_{BC}e^{-2h_B/r}}$

By this forward modeling use the digital filter coefficients of GOSH's filter in calculation. Then, can calculate the apparent resistivity as

$$\rho_a(r) = r^2 \int_0^\infty T(\lambda) J_1(r\lambda) \lambda d\lambda$$

And plot the apparent resistivity to pseudo dept.

2.1.1 Pseudo code for 1-D VES Forward modeling

Import Synthetic data or Observed data, Electrode spacing (L) and layers thickness (h)

Use Ghosh's digital Filter

Assign new L = 1/L

Calculate the dimension of distance (s),

$$s_{ij} = e^{-2h_i L_j}$$

Calculate the reflection coefficient (k),

$$k_{AB} = \frac{\rho_B - \rho_A}{\rho_B + \rho_A}$$

For range of h

Calculate the resistivity transform of n layer section (T_n),

$$T_n(r) = \frac{T'_{AB} + T_{n-1}}{1 + \frac{T'_{AB} T_{n-1}}{\rho_A^2}}$$

end

For Range of L

Calculate the apparent resistivity (ρ_a),

$$\rho_a(r) = r^2 \int_0^\infty T(\lambda) J_1(r\lambda) \lambda d\lambda$$

End

2.2 Inversion Algorithm

Inversion is a way to find a possible model of the earth that can generate predicted measurements that are similar to observations. It is the inverse of the forward modeling. In forward modeling, a given model is inputted and the predicted responses are generated. In an inversion, the observed data is inputted and the output is a model that generates data fitting the obtained data.

There are many inversion methods used in geophysics, such as the Quasi-Newton method (Trip et al., 1984), non-linear conjugate gradient (Newman et al., 2000), Levenberg-Marquardt method (Trip et al., 1984) and Occam's inversion (Constable et al., 1987).

Occam's inversion technique has been proposed by Constable et al. (1987) for solving the 1D resistivity inverse problem. Occam's inversion takes less iteration but uses more calculation time per iteration and more computer memory than other methods. Due to stability, in this project use Occam's inversion.

2.2.1 1D Occam's inverse

The philosophy of the Occam approach is to seek the smoothest or minimum structure model subject to a constraint on the misfit (see Constable et al., 1987; Siripanvaraporn & Egbert, 2000), which can be mathematically transformed into a problem of minimization of an objective function W,

$$\mathrm{W} = \Phi_{\mathrm{m}} + \lambda^{-1}\Phi_{\mathrm{d}}$$

when Φ_m is the model function. Φ_d is the data function. Here, we want to minimize Φ_m subject to $\Phi_m = 0$. λ is the Lagrange multiplier trade-off parameter between the model and data functions.

2.2.1.1 Data function

Data function is defined as

$$\Phi_d = \chi_d^2 - \chi_{d^*}^2$$

when χ_d^2 is the data misfit and $\chi_{d^*}^2$is the desired data. When the data misfit χ_d^2 is reduced to the desired misfit χ_{d*}^2, the data function $\Phi_d = 0$. As with the least-square problem, χ_d^2 represents an average variance between the measured data (d) and the numerically restricted data (f) which can be expressed by

$$\chi_d^2 = \sum_{i=1}^{N} \left(\frac{d_i - f_i}{\epsilon_i} \right)^2$$

when ϵ_i is the error of measured data d_i and N is the number of data. Can expressed the data misfit in matrix form as,

$$\chi_d^2 = (d - \mathrm{F}[m])^{\mathrm{T}} C_d^{-1} (d - \mathrm{F}[m])$$

when d is vector containing the measured data. F$[m]$ is a vector containing the predicted data generated by the forward modeling from the model vector m (F represents the forward modeling operator),

$$\mathrm{F}[m] = \begin{bmatrix} f_1 \\ f_2 \\ f_3 \\ \vdots \\ f_N \end{bmatrix}_{N \times 1} \quad \text{and } m = \begin{bmatrix} \rho_1 \\ \vdots \\ \rho_M \end{bmatrix}_{M \times 1}$$

when M is the number of model parameters which equal to the total number of discretized model blocks. The inverse data covariance matrix can be expressed as

$$C_d^{-1} = W_d^{\mathrm{T}} W_d$$

where

$$W_d = \begin{bmatrix} 1/\epsilon_1 & & & \\ & 1/\epsilon_2 & & \\ & & \ddots & \\ & & & 1/\epsilon_N \end{bmatrix}_{N \times N}$$

2.2.1.2 Model function

Here, for Occam's inversion, the smoothness constraint is assumed according to the philosophy of minimum structure. The model function $\Phi_m$is then estimated by the smoothness of the model represented by the model norm $\chi_m^2$and defined as an average variance of the model parameter between the consecutive discretized blocks.

$$\Phi_m = \chi_m^2 - \chi_{m^*}^2$$

χ_m^2 can be expressed by

$$\chi_m^2 = \sum_{i=1}^{M} (m_{i+1} - m_i)^2$$

The model norm can be written in matrix form as,

$$\chi_m^2 = (m_{k+1} - m_0)^{\mathrm{T}} C_m^{-1} (m_{k+1} - m_0)$$

when m_0 is the reference prior model, C_m is the model covariance. The model roughness or the inverse of the model covariance (C_m^{-1}) operator can write as,

$$C_m^{-1} = \Delta_z^{\mathrm{T}} \Delta_z$$

when Δ_z which the vertical roughening matrix which operate on a 1D model and M_z is number of model layers.

$$\Delta_z = \begin{bmatrix} 0 & & & & \\ -1 & 1 & & & \\ & -1 & 1 & & \\ & & \ddots & \ddots & \\ & & & -1 & 1 \end{bmatrix}_{M_z \times M_z}$$

2.2.1.3 Minimization of objective function

For Occam's inversion the objective function can be expressed according to the given data function and model as,

$$W(\lambda, m) = (m - m_0)^{\mathrm{T}} C_m^{-1} (m - m_0) + \lambda^{-1} \left[(d - \mathrm{F}[m])^{\mathrm{T}} C_d^{-1} (d - \mathrm{F}[m]) - \chi_{d^*}^2 \right]$$

when $\chi_{d*}^2$is the desired level of misfit.

Form the Taylor's series expansion to linearize F[m].

$$\mathrm{F}[m + \Delta m] = \mathrm{F}[m] + \frac{\partial \mathrm{F}[m]}{\partial m} \Delta m$$

Since $m_{k+1} = m_k + \Delta m$, equation above can be written in iterative form,

$$\mathrm{F}[m_{k+1}] = \mathrm{F}[m_k] + J_k (m_{k+1} - m_k),$$

when *k* denotes the iteration number, m_{k+1} represents the model at the next iteration, and the first derivative J_k is the Jacobian or sensitivity calculated at iteration *k* and

$$J_k \equiv \frac{\partial \mathrm{F}[m]}{\partial m},$$

$$J_k = \begin{bmatrix} \frac{F[m + \rho_1]_1 - F[m]_1}{\rho_1} & \cdots & \frac{F[m + \rho_l]_1 - F[m]_1}{\rho_l} \\ \vdots & \ddots & \vdots \\ \frac{F[m + \rho_1]_N - F[m]_N}{\rho_1} & \cdots & \frac{F[m + \rho_l]_N - F[m]_N}{\rho_l} \end{bmatrix}_{N \times l}$$

when *N* is number of data and l is number of model layer.

Get the objective function in iterative form,

$$W_\lambda = (m_{k+1} - m_0)^{\mathrm{T}} C_m^{-1} (m_{k+1} - m_0) + \lambda^{-1} \Big[\big(d - \mathrm{F}[m_k] - J_k (m_{k+1} - m_k) \big)^{\mathrm{T}} C_d^{-1} \big(d - \mathrm{F}[m_k] - J_k (m_{k+1} - m_k) \big) - \chi_{d^*}^2 \Big].$$

To incorporate the prior model m_0 into the inversion, replace as

$$m_{k+1} - m_k = (m_{k+1} - m_0) - (m_k - m_0)$$

The objective function becomes

$$W_\lambda = (m_{k+1} - m_0)^{\mathrm{T}} C_m^{-1}(m_{k+1} - m_0) + \lambda^{-1}\left[\left(\hat{d} - J_k(m_{k+1} - m_0)\right)^{\mathrm{T}} C_d^{-1}\left(\hat{d} - J_k(m_{k+1} - m_0)\right) - \chi^2_{d^*}\right],$$

when $\hat{d} = d - \mathrm{F}[m_k] + J_k(m_k - m_0)$.

In order to find the m_{k+1} that minimizes the objective function, we differentiate equation above with respect to m_{k+1} at the stationary point,

$$\frac{\partial W_\lambda}{\partial m_{k+1}} = 0.$$

Hence, the expression of the iterative sequence is

$$m_{k+1} = (\lambda C_m^{-1} + \Gamma_k^m)^{-1} J_k^T C_d^{-1} \hat{d} + m_0,$$

when $\Gamma_k^m = J_k^T C_d^{-1} J_k$.

2.2.2 Pseudo code for Occam's inversion

Import synthetic data or observed data, error of each data

Assign initial model or m_0 Lagrange multiplier (λ)

Calculate the C_m^{-1}, C_d^{-1} and first Jacobian matrix

Define m_1 by using $m_k = m_0$

for Range of Lagrange multiplier (λ)

Choose the λ that give the lowest data misfit

end

Calculate m_{k+1} first iteration from

$$m_{k+1} = (\lambda C_m^{-1} + \Gamma_k^m)^{-1} J_k^T C_d^{-1} \hat{d} + m_0$$

for second iteration to the iteration that m_{k+1} satisfy some condition

Update F[m]

Calculate new Jacobian matrix

Find new Lagrange multiplier

Calculate m_{k+1} from

$m_{k+1} = (\lambda C_m^{-1} + \Gamma_k^m)^{-1} J_k^T C_d^{-1} \hat{d} + m_0$

end

2.3 Chapter Summary

This chapter has discussed background knowledge for the forward modeling and inversion process. The content has covered the 1D VES forward modeling and 1D VES inversion which used to image the 1D subsurface resistivity model. This chapter is preparation for the next chapter in which the detail of 1D VES inversion development and lateral constraint will be discussed.

Chapter 3

Methodology

The inverse modeling for one-dimension VES is the synchronization of knowledge which had discussed previously. This chapter will explain all processes of calculation and adaptation about adding lateral constraint from the brief overall process to deep detail of each topic.

3.1 Overall Process

The calculation and prediction of the subsurface resistivity model of one-dimensional Vertical Electrical Sounding survey inversion are sophisticated, hence, the overall process is stated first to clear the idea methodology of this research.

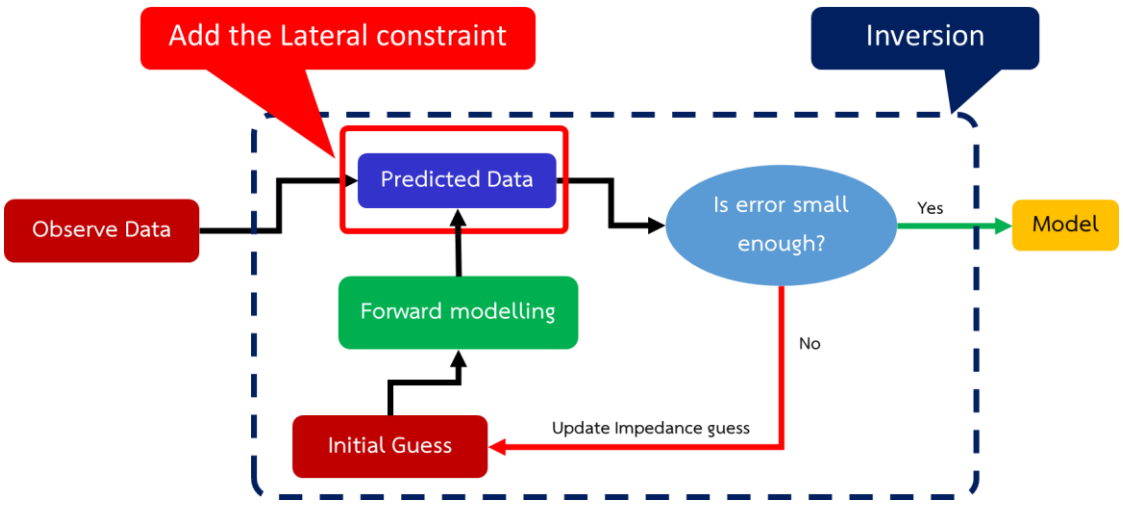

Figure 3.1 : Position of adding the Lateral constraint

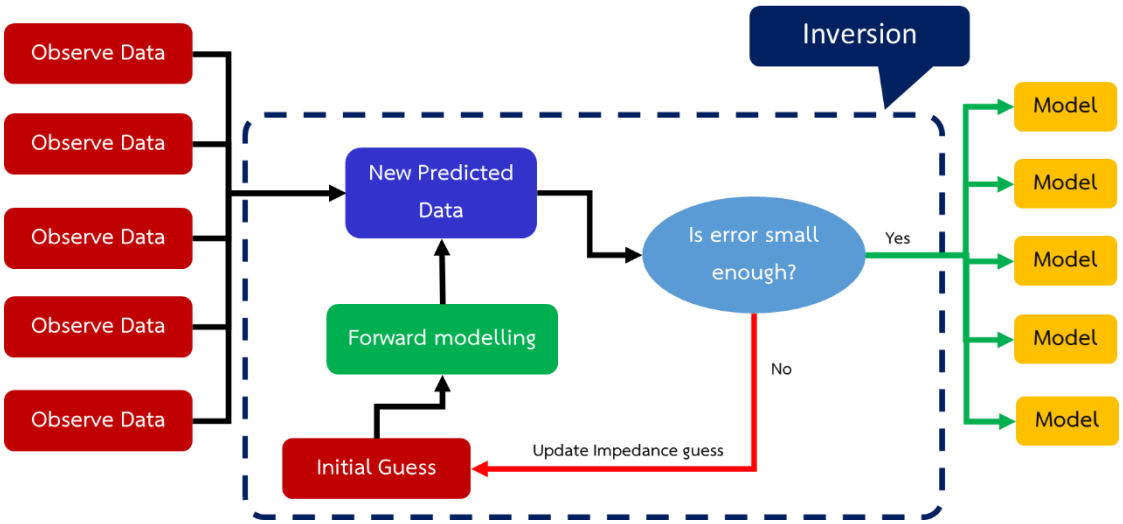

Figure 3.2 : Inversion process with Lateral constraint

The objective is an adaptation of the optimization in the predicted data section of the inversion system by modifying the model covariance (C_m) or model roughness (C_m^{-1}) of 1D VES inversion.

Normally, the model covariance (C_m) or roughness operator (C_m^{-1}) of 1D VES inversion is calculated only z-dimension or the vertical, on the other hand, x-dimension is not calculated because the 1D VES acquired data is usually performed individually for each station. So, the 1D VES inversion predict the earth's model to multiple layers in vertical and obtain the result is the subsurface resistivity model which show the predicted layer earth's model but the obtained model can totally differ for the obtained model from 1D VES for the nearby station because of the limitation of 1D inversion.

This research interest is integrating the data of nearby VES sites station into the model covariance (C_m) or model roughness (C_m^{-1}) of 1D VES inversion by with the assumption that the geological structure would not have the roughly change or don't differ together too much.

Due to the model roughness is important for lateral constraint, so this focuses on the modifying of the model roughness which integrates the acquire data of nearby 1D VES site stations and called Lateral constraint.

3.2 Lateral Constraint

From the 1D VES inversion which the acquired data from the investigation is usually performed individually for each station, so, the model covariance (C_m) or model roughness (C_m^{-1}) can be predicted the model only z-dimension. The model roughness or the inverse of the model covariance (C_m^{-1}) operator of 1D VES inversion that previously mentioned can write as,

$$C_m^{-1} = \Delta_z^{\mathrm{T}} \Delta_z$$

when Δ_z which the vertical roughening matrix which operate on a 1D model.

Thus, from the idea that integrating the acquired data of nearby 1D VES site stations into the optimization part of the 1D inversion system to weigh the obtained model from data of nearby stations, the model roughness has to modify to calculate other stations together. Moreover, the updated model roughness has to can calculate and predict the subsurface resistivity model at horizontal or x-dimension of the stations.

From the reasons above, the model roughness that can calculate and predict the model from z-dimension and x-dimension or vertical and horizontal side of the station is the model roughness of the 2D inversion system. Thus, the model roughness from the 2D inversion system is adapted to the 1D inversion system can write as

$$C_m^{-1} = \Delta x^T \Delta x + \Delta z^T \Delta z$$

when $C_m^{-1}$is model roughness or the inverse of the model covariance operator which is introduced in Degroot-Hedlin & Constable (1990) and Puwis er al. (2010), Δx is horizontal roughening matrix and Δz is the vertical roughening matrix which both are the operate on a 2D model with an assumed y strike direction.

For the adaptation of the model roughness of 2D inversion into the 1D inversion so, the new model roughness which is used for adding lateral is interpreted like the 2D by data of the horizontal come from the nearby stations. For the example of the 1D model that joint with the 1D model of nearby stations is consisting of $M_x$element in the x-direction or the number of joint stations, $M_z$elements in z-direction and $M = M_x \times M_z$, Δx can be expressed as

$$\Delta_x = \begin{bmatrix} -1 & \cdots & 1 & & \cdots \\ & -1 & \cdots & 1 & \cdots \\ & \ddots & & \ddots & \\ \cdots & & -1 & \cdots & 1 \\ & & 0 & & \end{bmatrix}_{M \times M}$$

where 0 is $M_z \times M$ zero matrix. The vertical roughening matrix (Δz) can rewrite as

$$\Delta_z = \begin{bmatrix} \Delta_1 & & & \\ & \Delta_2 & & \\ & & \ddots & \\ & & & \Delta_{M_z} \end{bmatrix}_{M \times M}$$

where Δ_i is the $M_x \times M_x$ vertical roughening sub-matrix for the column of grid i as,

$$\Delta_i = \begin{bmatrix} 0 & & & & \\ -1 & 1 & & & \\ & -1 & 1 & & \\ & & \ddots & \ddots & \\ & & & -1 & 1 \end{bmatrix}_{M_x \times M_x}$$

3.3 Other Operators Which Has Been Modified

After the adaptation of the model roughness, many operators of the 1D VES inversion system have to modify to a new form for calculating many stations together.

3.3.1 Measured and Predicted data matrices

For 1D VES inversion process, the measured data (d) and predicted data ($F[m]$) were contained in matrices form as

$$d = \begin{bmatrix} \rho_1 \\ \rho_2 \\ \rho_3 \\ \vdots \\ \rho_N \end{bmatrix}_{N\times 1} \quad \text{and} \quad \mathrm{F}[m] = \begin{bmatrix} f_1 \\ f_2 \\ f_3 \\ \vdots \\ f_N \end{bmatrix}_{N\times 1}$$

when d is a vector containing the measured data. $\mathrm{F}[m]$ is a vector containing the predicted data generated by the forward modeling and N is the number of acquired data.

For the co-calculation many stations in 1D VES inversion, the measured data and predicted data matrices rewrite as

$$d = \begin{bmatrix} d_1 \\ d_2 \\ \vdots \\ d_n \end{bmatrix}_{(nN)\times 1} \quad \text{and} \quad \mathrm{F}[m] = \begin{bmatrix} \mathrm{F}[m_{d_1}] \\ \mathrm{F}[m_{d_2}] \\ \vdots \\ \mathrm{F}[m_{d_n}] \end{bmatrix}_{(nN)\times 1}$$

when n is the number of stations in the calculation, d is the vector containing the measured data of each station and $\mathrm{F}[m]$ is a vector containing the predicted data of each model's stations which expressed as

$$d_i = \begin{bmatrix} \rho_1 \\ \rho_2 \\ \rho_3 \\ \vdots \\ \rho_N \end{bmatrix}_{N\times 1} \quad \text{and} \quad \mathrm{F}\left[m_{d_i}\right] = \begin{bmatrix} f_1 \\ f_2 \\ f_3 \\ \vdots \\ f_N \end{bmatrix}_{N\times 1}$$

3.3.2 The inverse data covariance matrix (C_d^{-1})

The inverse data covariance matrix of 1 station for 1D inversion process can be obtained from

$$C_d^{-1} = W_d^{\mathrm{T}} W_d$$

where the inverse data covariance sub-matrix (W_d)

For co-calculation of many stations, the inverse data covariance matrix use the same form but the inverse data covariance sub-matrix (W_d) can rewrite that

$$W_d = \begin{bmatrix} W_{d_1} & & & \\ & W_{d_2} & & \\ & & \ddots & \\ & & & W_{d_n} \end{bmatrix}_{nN \times nN}$$

when n is number of stations, W_{d_i} is the inverse data covariance sub-matrix of each stations write as

$$W_{d_i} = \begin{bmatrix} 1/\epsilon_1 & & & \\ & 1/\epsilon_2 & & \\ & & \ddots & \\ & & & 1/\epsilon_N \end{bmatrix}_{N \times N}$$

when ϵ_i is the error of measured data d_i and N is the number of data.

3.3.3 Jacobian matrix

The sensitivity or Jacobian matrix at iteration k of 1 station for 1D VES inversion system obtained from

$$J_k \equiv \frac{\partial \mathrm{F}[m]}{\partial m},$$

$$J_k = \begin{bmatrix} \frac{F[m+\rho_1]_1 - F[m]_1}{\rho_1} & \cdots & \frac{F[m+\rho_l]_1 - F[m]_1}{\rho_l} \\ \vdots & \ddots & \vdots \\ \frac{F[m+\rho_1]_N - F[m]_N}{\rho_1} & \cdots & \frac{F[m+\rho_l]_N - F[m]_N}{\rho_l} \end{bmatrix}_{N \times l}$$

For co-calculation of many stations, the Jacobian matrix use the same form in each station but modify the cooperation Jacobian matrix as

$$J_k = \begin{bmatrix} J_{k1} & & \\ & J_{k2} & \\ & & \ddots \\ & & & J_{kn} \end{bmatrix}_{nN \times nl}$$

when n is the number of stations, N is the number of data and l is number of model's layer.

3.4 Chapter Summary

This chapter started with the overall process of the idea, then the detail of each process was discussed. The details cover modifying the Lateral constraint and other parameters and operators which have been modified. The methodology, idea, and assumption are all explained, the next chapter is about validation to check the reliability of this project result.

Chapter 4

Results and Discussion

In this chapter, we apply the developed inversion with the lateral constraint to synthetic and real data. The results from the development of 1D VES inversion with lateral constraint will be shown in the first part. Then, the results of applying the real data from geophysics exploration at Sai Yok, Kanchanaburi, Thailand will be shown in the second part.

4.1 Synthetic Experiments

This research aims to develop a 1D VES inversion code by adding the lateral constraint. The results of the developed program in some synthetic data cases will show in this part.

Sets of the synthetic data are generated from synthetic models using 1D VES forward modeling techniques. The calculated data are then treated as the observed data.

4.1.1 Synthetic case I : 2 layers

4.1.1.1 Joint 2 stations

4.1.1.1.1 Synthetic data and model

The synthetic models are [100 10,000] and [300 15,000], both stations have the same thickness as 50 meters and the same electrode spacing which is shown in Figure 4.1.

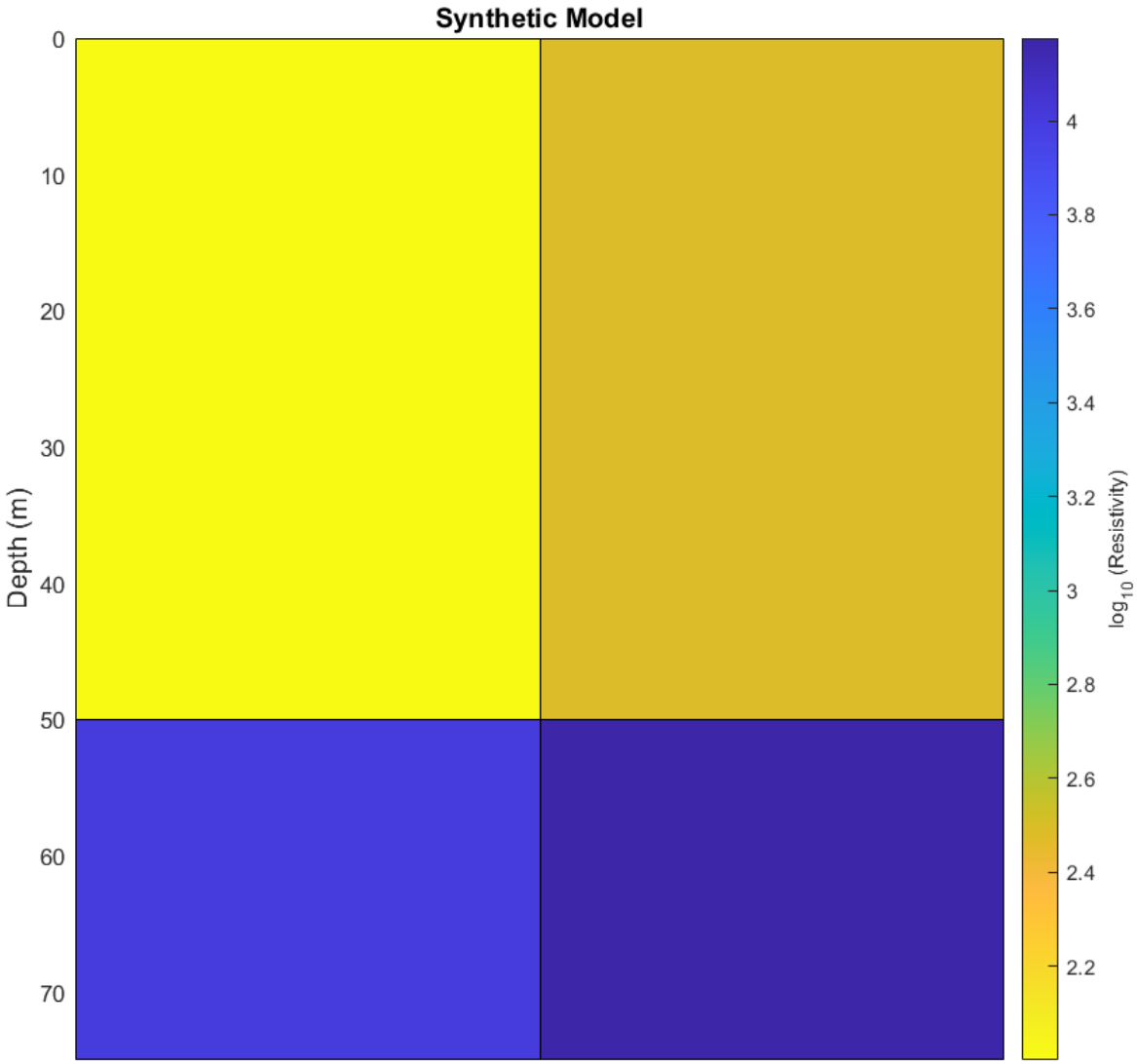

Figure 4.1 : Synthetic model of 2 layers case of station 1 (left) and 2 (right)

4.1.1.1.2 Inversion result

Figure 4.2 shows the apparent resistivity transform VS electrode spacing (AB/2) and mean relative error from synthetic data and calculated data which update from the initial response of synthetic data in section 4.1.1.1.1.

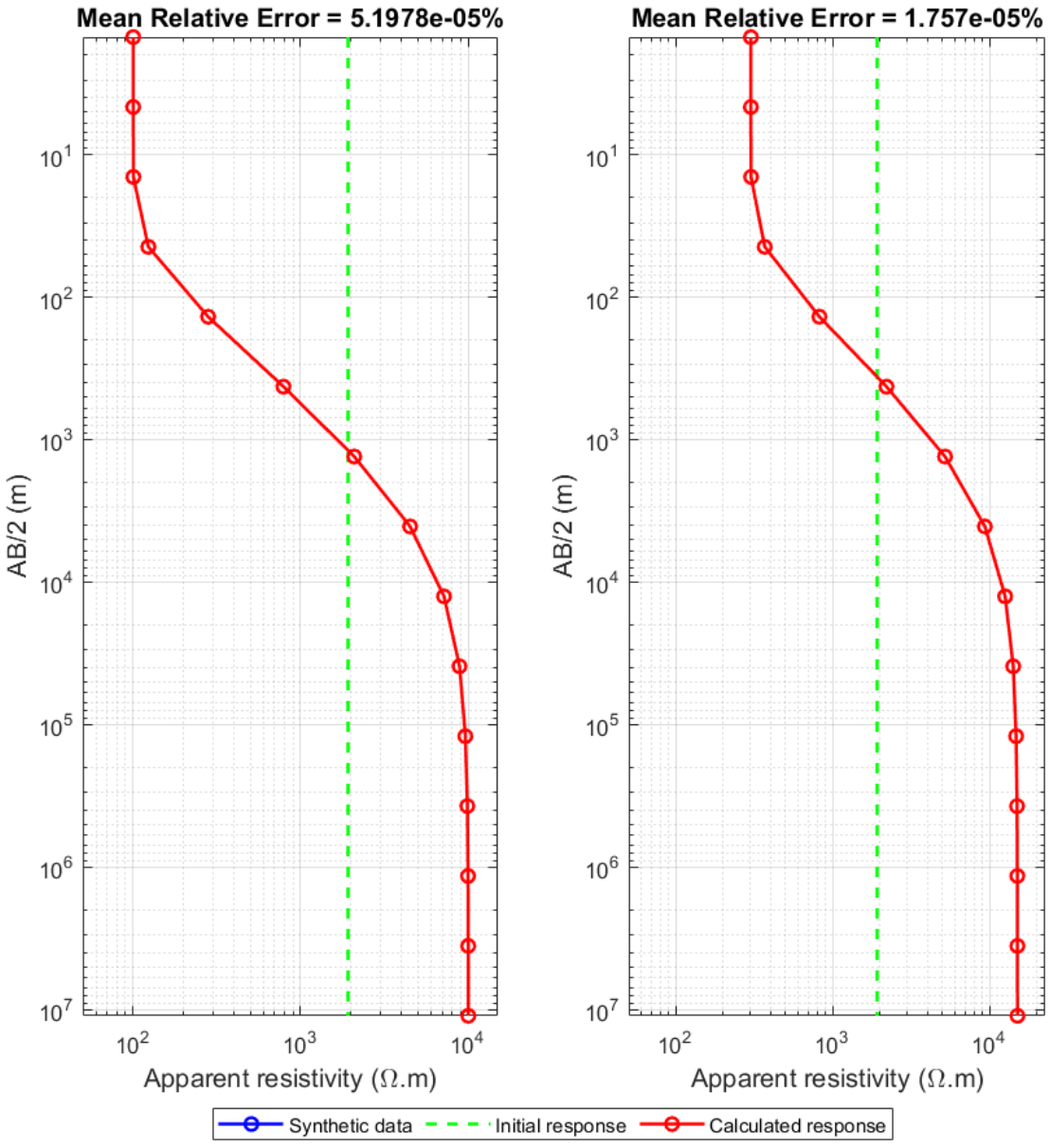

Figure 4.2 : Resistivity transform of synthetic 2 layers case joint with station 1 (left) and 2 (right)

Figure 4.3 shows the resistivity model with the pseudo depth of synthetic model and calculated model which update from the initial model and the number of iterations calculation of synthetic data in section 4.1.1.1.1.

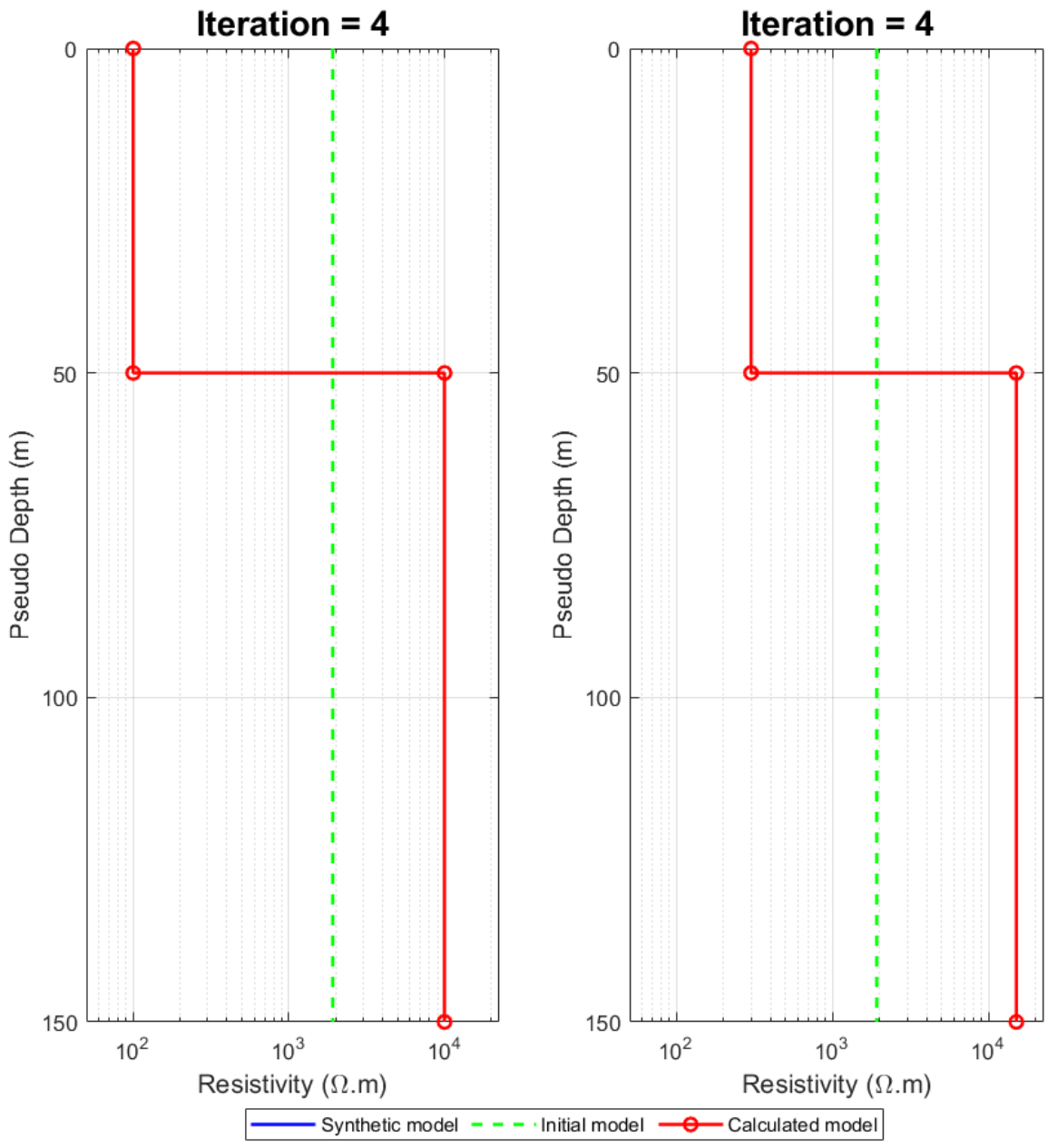

Figure 4.3 : Resistivity model of synthetic 2 layers case joint with station 1 (left) and 2 (right)

Figure 4.4 shows the calculated model which is the result from developed 1D VES program of synthetic data in section 4.1.1.1.1.

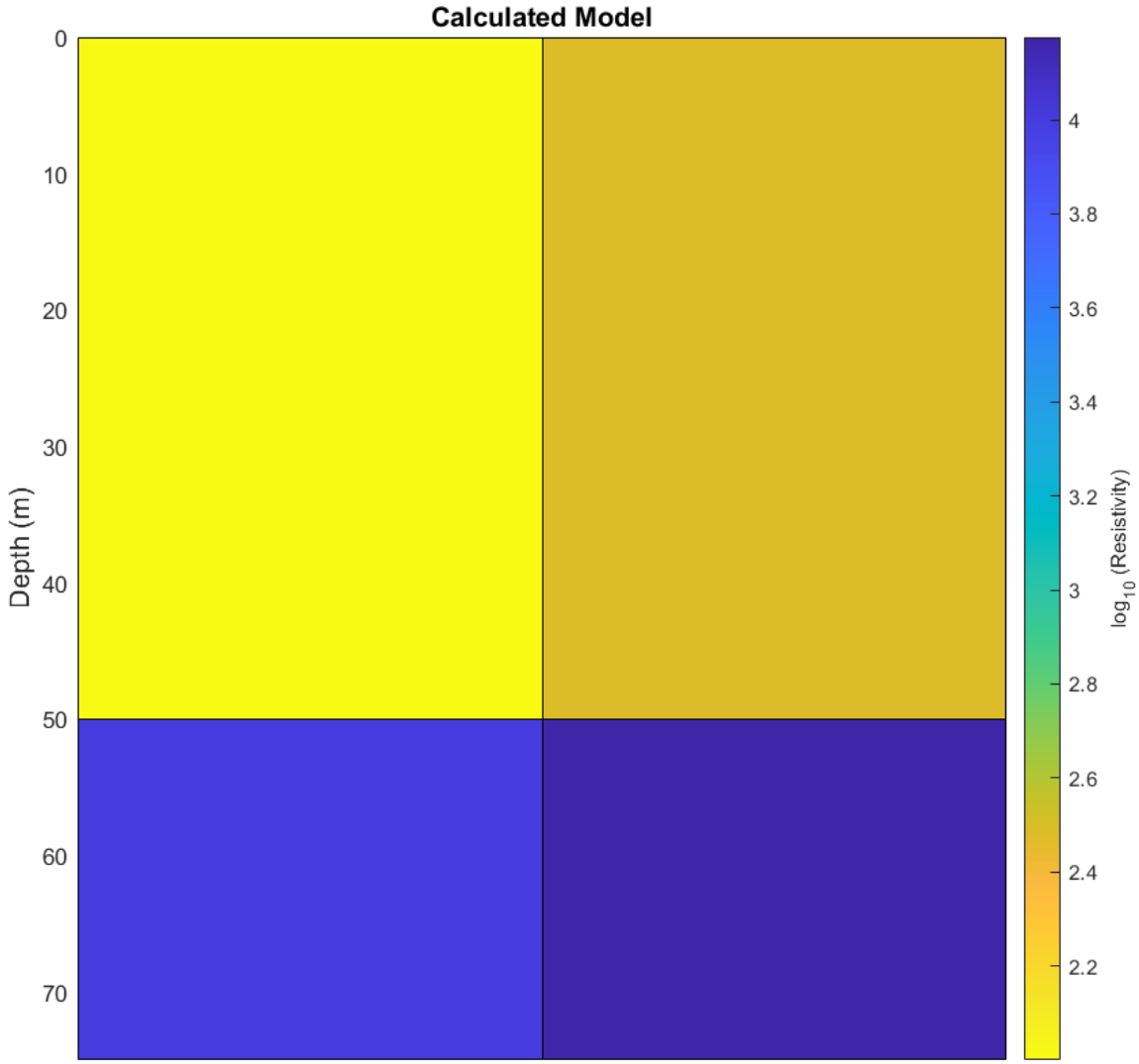

Figure 4.4 : Calculated model of 2 layers case of station 1 (left) and 2 (right)

4.1.1.2 Joint 6 stations

4.1.1.2.1 Synthetic data and model

The synthetic models are matrices [100 10,000], [300 15,000], [500 13,000], [200 20,000], [150 10,000], and [450 14,000], all of the models' stations have the same thickness as 50 meters and the same electrode spacing which is shown in Figure 4.5.

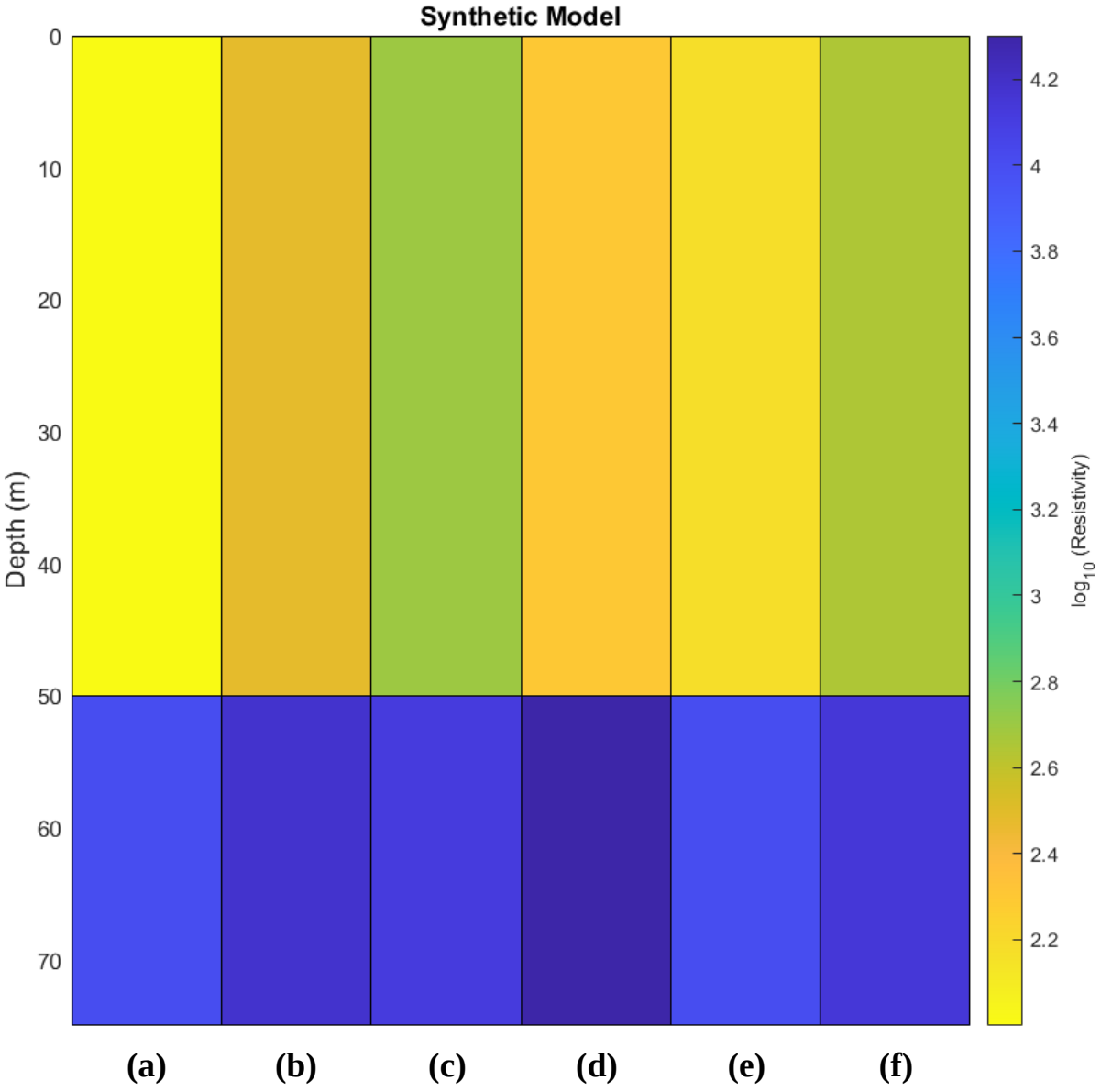

Figure 4.5 : Synthetic model of synthetic 2 layers case joint with station 1 (a), 2 (b), 3 (c), 4 (d), 5 (e) and 6 (f)

4.1.1.2.2 Inversion result

Figure 4.6 shows the apparent resistivity transform VS electrode spacing (AB/2) and mean relative error from synthetic data and calculated data which update from the initial response of synthetic data in section 4.1.1.2.1.

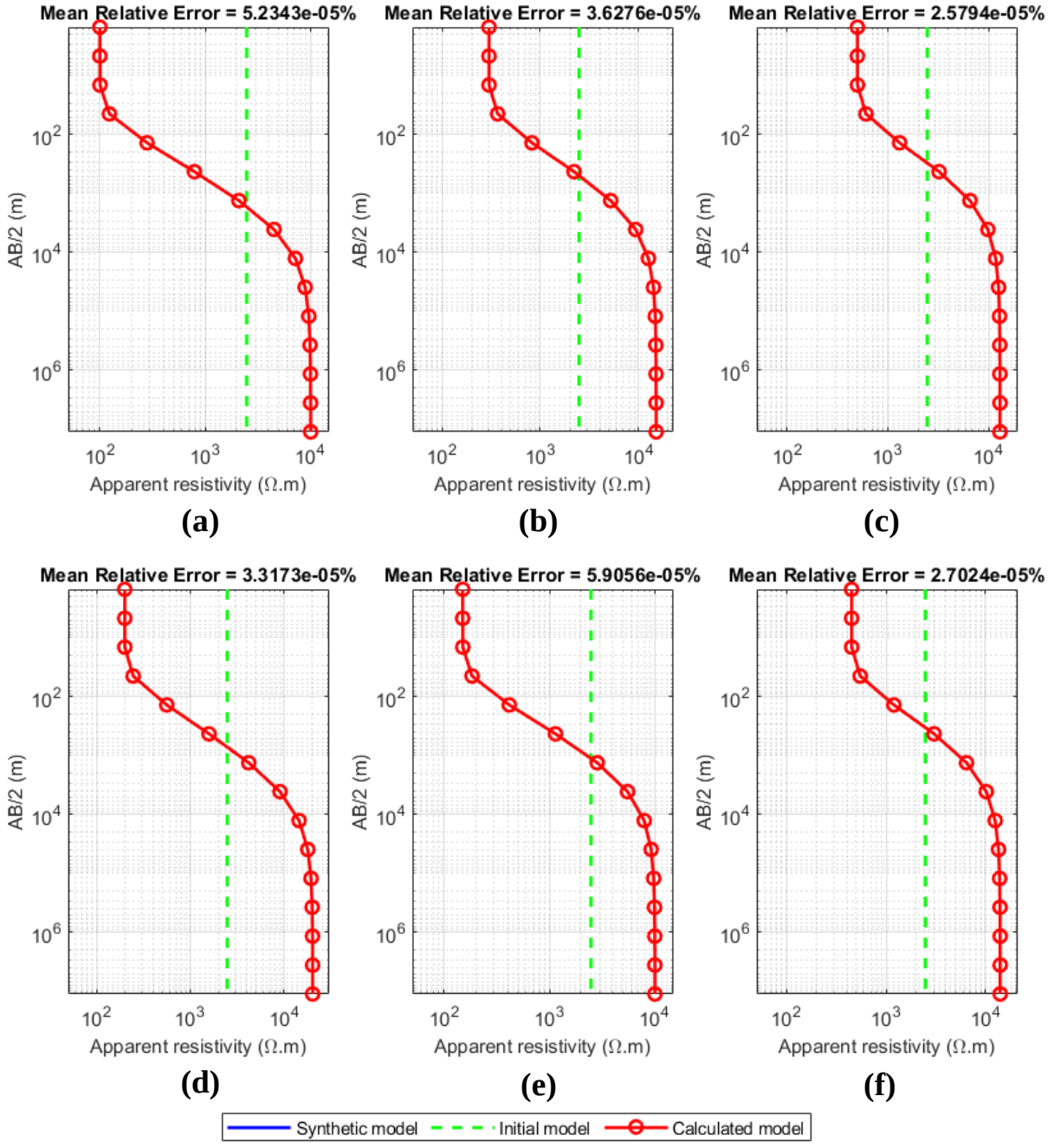

Figure 4.6 : Resistivity transform of synthetic 2 layers case joint with station 1 (a), 2 (b), 3 (c), 4 (d), 5 (e) and 6 (f)

Figure 4.7 shows the resistivity model with the pseudo depth of synthetic model and calculated model which update from the initial model and the number of iterations calculation of synthetic data in section 4.1.1.2.1.

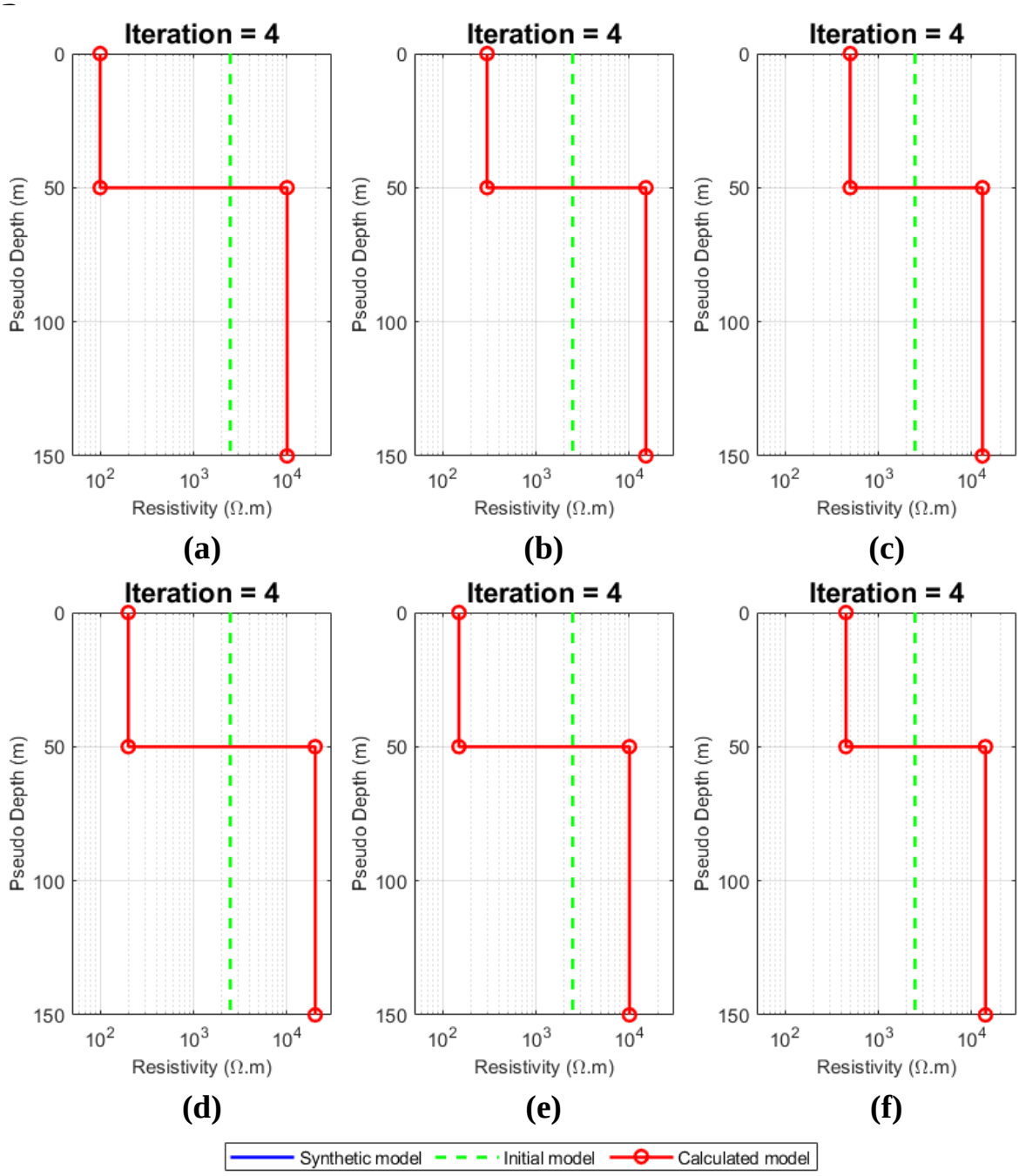

Figure 4.7 : Resistivity model of synthetic 2 layers case joint with station 1 (a), 2 (b), 3 (c), 4 (d), 5 (e) and 6 (f)

Figure 4.8 shows the calculated model which is the result from developed 1D VES program of synthetic data in section 4.1.1.2.1.

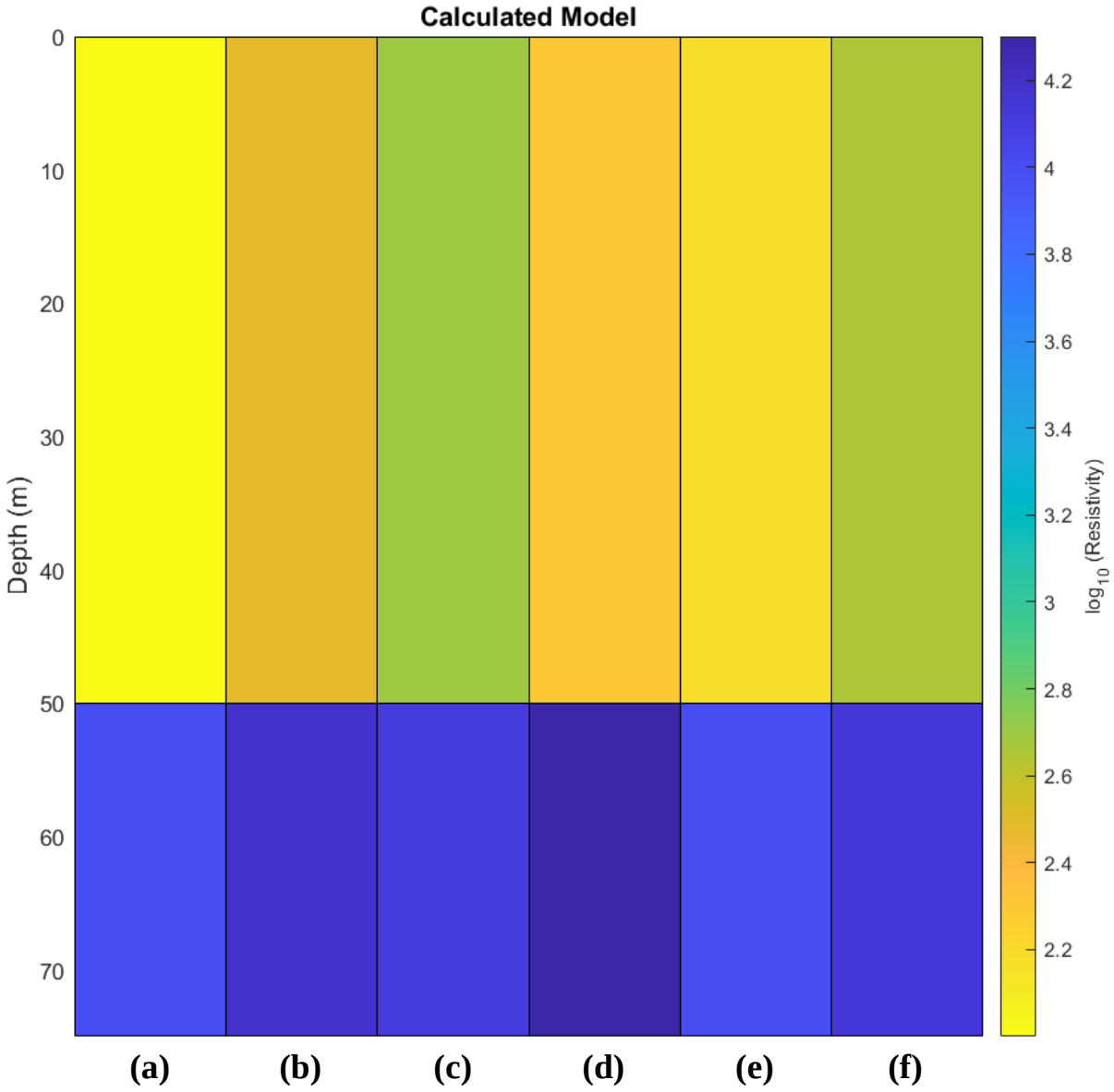

Figure 4.8 : Calculated model of synthetic 2 layers case joint with station 1 (a), 2 (b), 3 (c), 4 (d), 5 (e) and 6 (f)

4.1.1.3 Joint 9 stations

4.1.1.3.1 Synthetic data and model

The synthetic models are matrices [100 10,000], [300 15,000], [500 13,000], [200 20,000], [150 10,000], [450 14,000], [700 16,000], [650 18,500], and [550 19,000], all of the models' stations have the same thickness as 50 meters and the same electrode spacing which is shown in Figure 4.9.

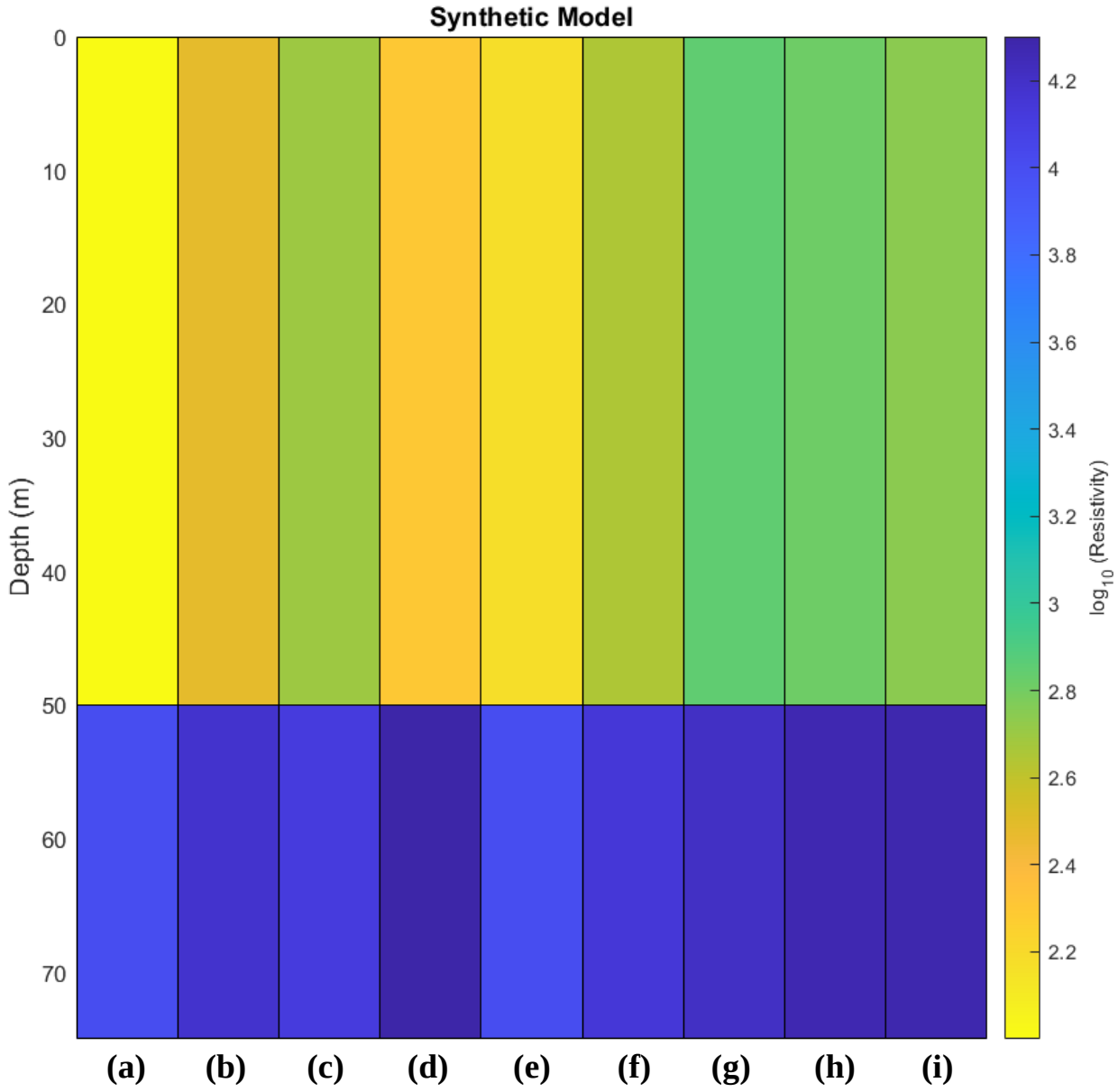

Figure 4.9 : Synthetic model of synthetic 2 layers case joint with station 1 (a), 2 (b), 3 (c), 4 (d), 5 (e), 6 (f), 7 (g), 8 (h) and 9 (i)

4.1.1.3.2 Inversion result

Figure 4.10 shows the apparent resistivity transform VS electrode spacing (AB/2) and mean relative error from synthetic data and calculated data which update from the initial response of synthetic data in section 4.1.1.3.1.

Figure 4.11 shows the resistivity model with the pseudo depth of synthetic model and calculated model which update from the initial model and the number of iterations calculation of synthetic data in section 4.1.1.3.1.

Figure 4.12 shows the calculated model which is the result from developed 1D VES program of synthetic data in section 4.1.1.3.1.

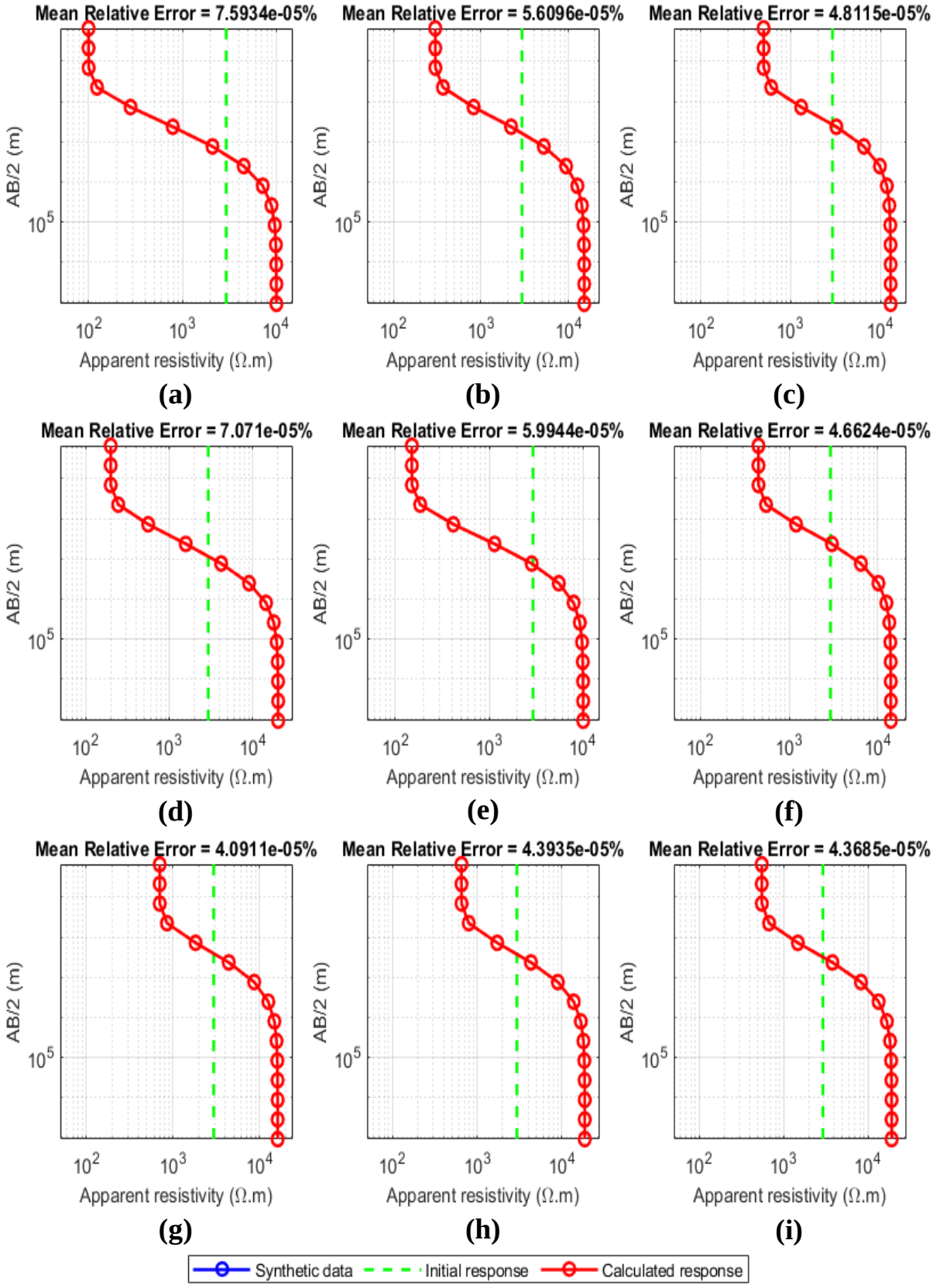

Figure 4.10 : Resistivity transform of synthetic 2 layers case joint with station 1 (a), 2 (b), 3 (c), 4 (d), 5 (e), 6 (f), 7 (g), 8 (h) and 9 (i)

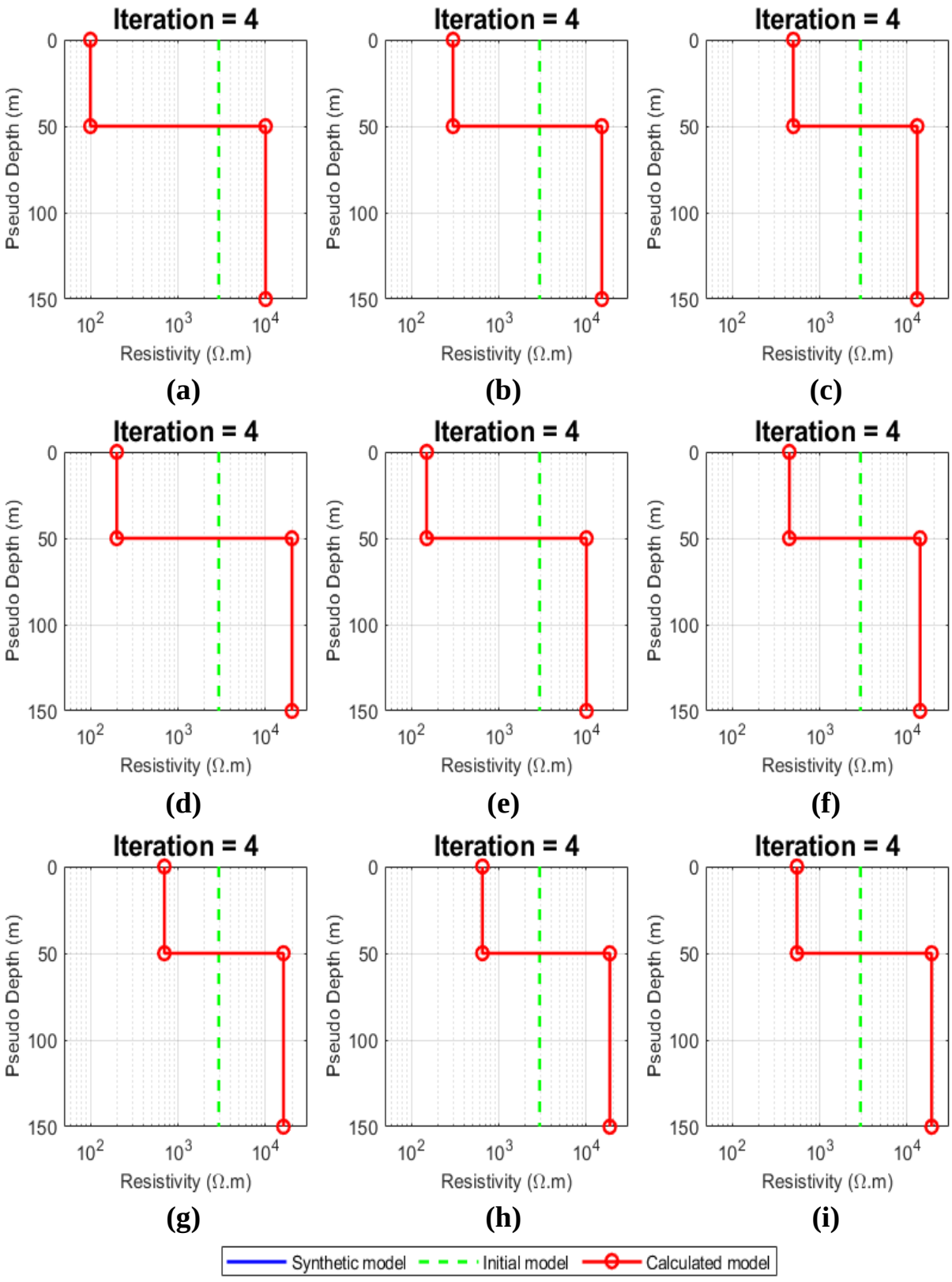

Figure 4.11 : Resistivity model of synthetic 2 layers case joint with station 1 (a), 2 (b), 3 (c), 4 (d), 5 (e), 6 (f), 7 (g), 8 (h) and 9 (i)

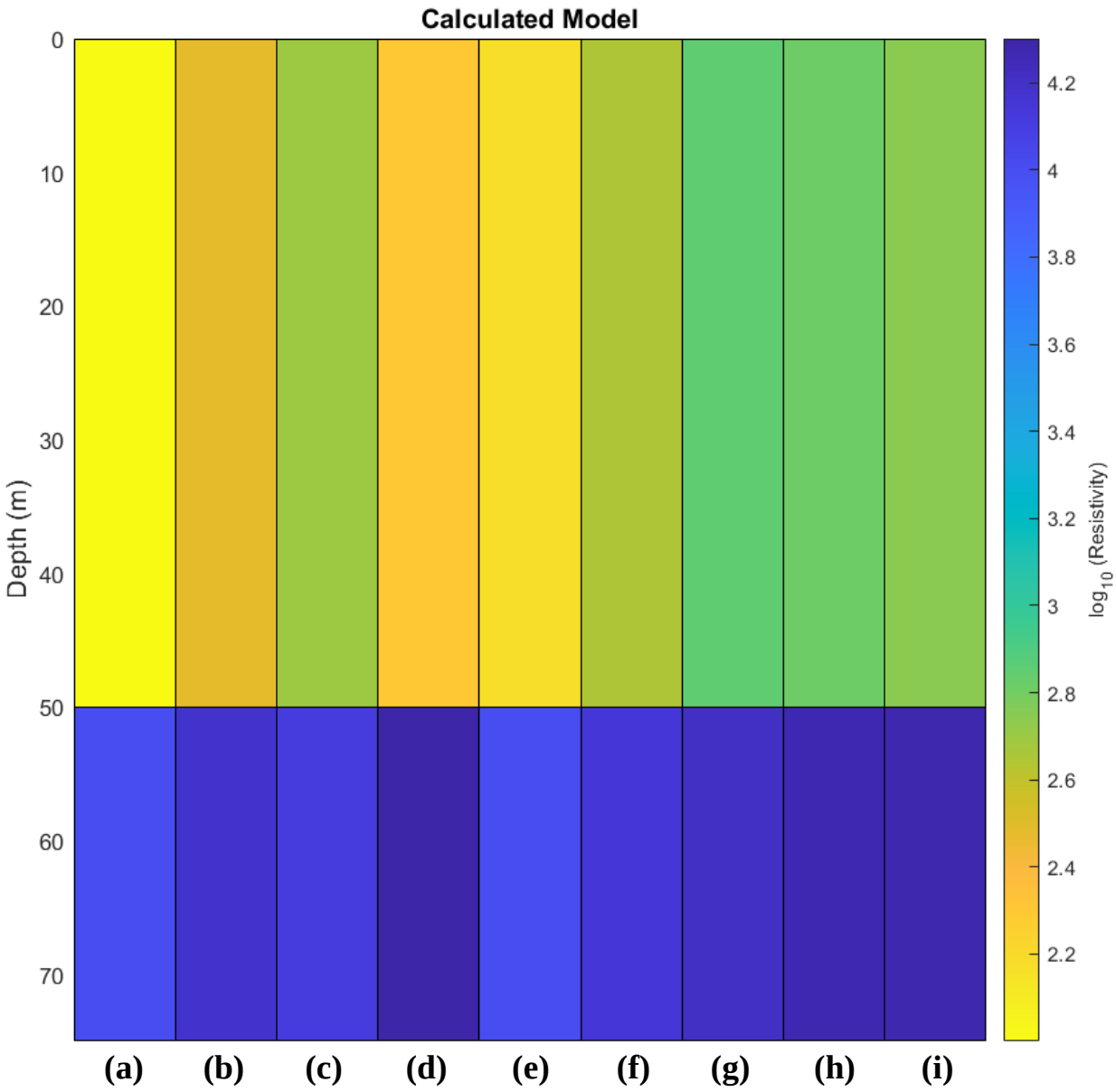

Figure 4.12 : Calculated model of synthetic 2 layers case joint with station 1 (a), 2 (b), 3 (c), 4 (d), 5 (e), 6 (f), 7 (g), 8 (h) and 9 (i)

4.1.2 Synthetic case II : 6 layers

4.1.2.1 Joint 2 stations

4.1.2.1.1 Synthetic data and model

The synthetic models are [100 100 1,000 1,000 10,000 10,000] and [500 500 5,000 5,000 50,000 50,000], both stations have the same thickness matrices as [20 20 50 50 80] meters and the same electrode spacing which is shown in Figure 4.13.

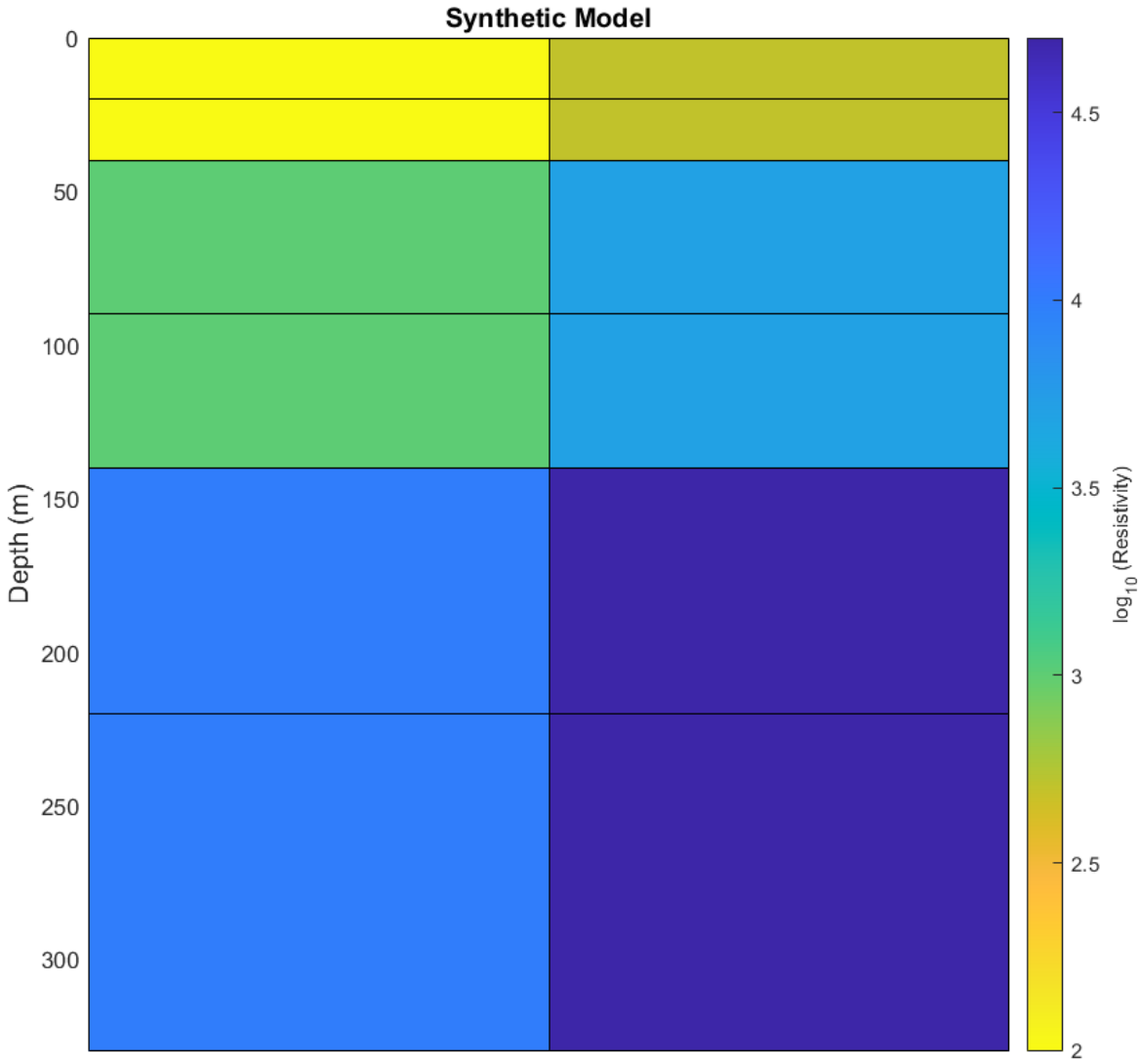

Figure 4.13 : Synthetic model of 6 layers case of station 1 (left) and 2 (right)

4.1.2.1.2 Inversion result

Figure 4.14 shows the apparent resistivity transform VS electrode spacing (AB/2) and mean relative error from synthetic data and calculated data which update from the initial response of synthetic data in section 4.1.2.1.1.

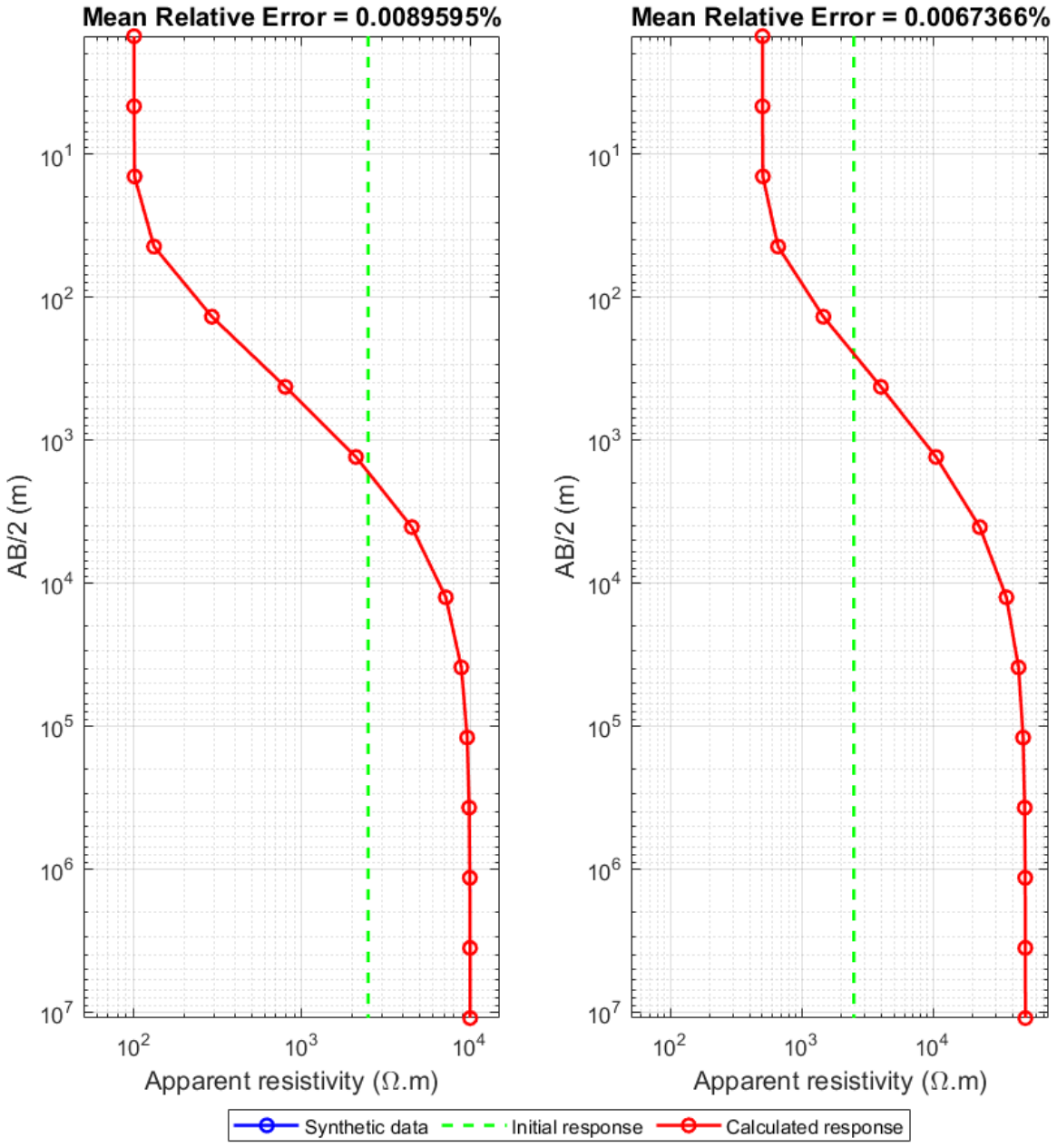

Figure 4.14 : Resistivity transform of synthetic 6 layers case joint with station 1 (left) and 2 (right)

Figure 4.15 shows the resistivity model with the pseudo depth of synthetic model and calculated model which update from the initial model and the number of iterations calculation of synthetic data in section 4.1.2.1.1.

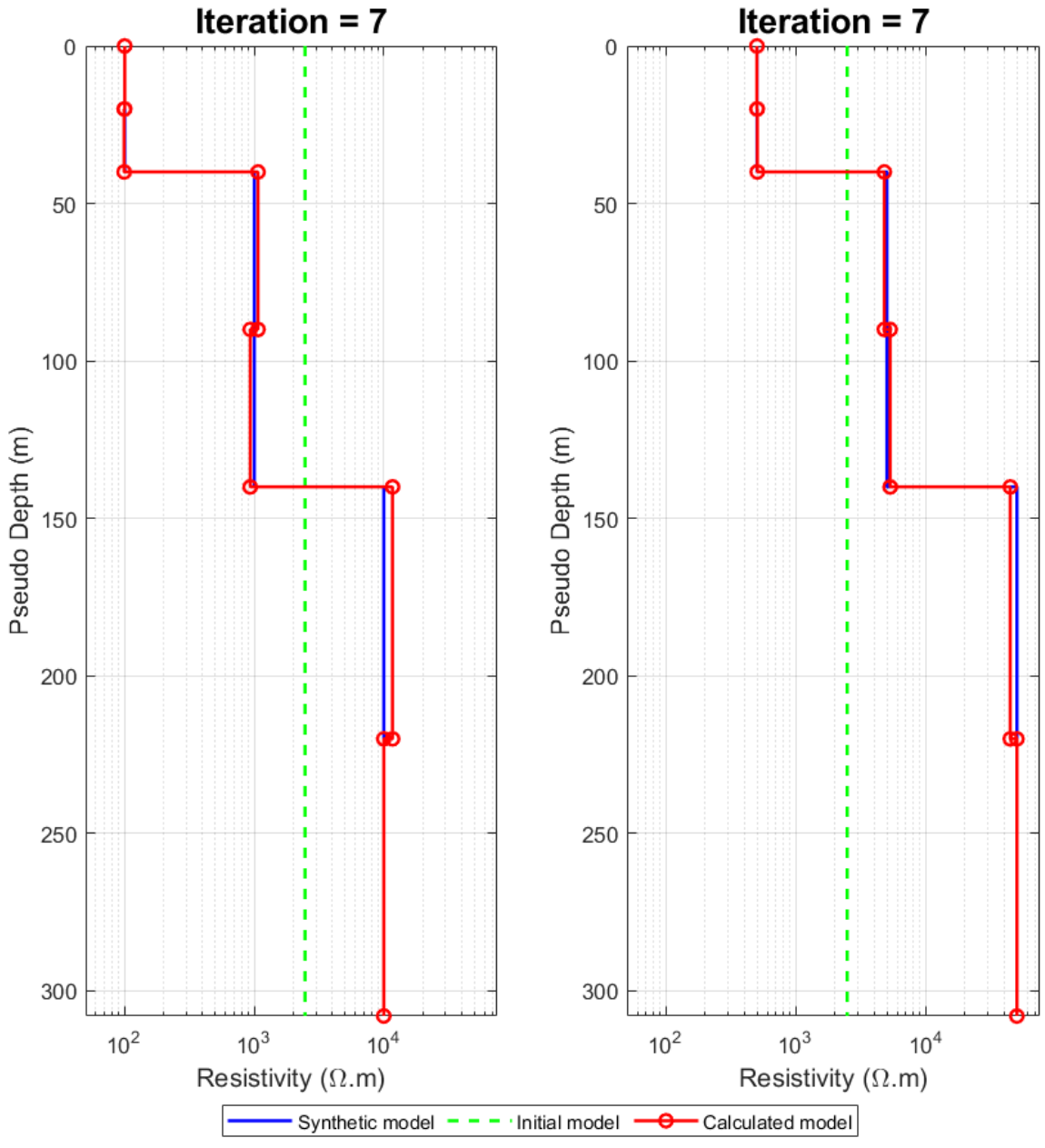

Figure 4.15 : Resistivity model of synthetic 6 layers case joint with station 1 (left) and 2 (right)

Figure 4.16 shows the calculated model which is the result from developed 1D VES program of synthetic data in section 4.1.2.1.1.

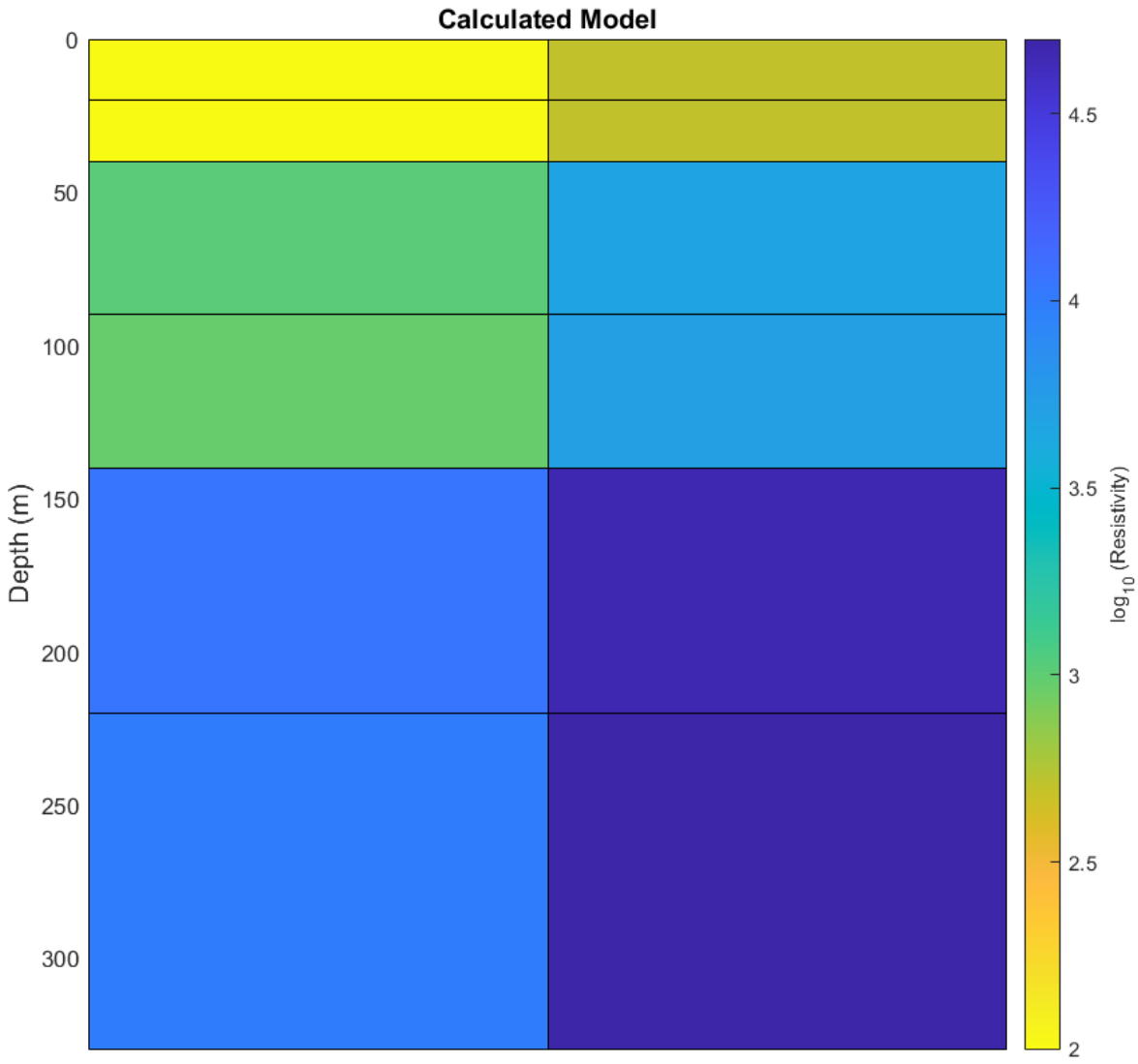

Figure 4.16 : Calculated model of 6 layers case of station 1 (left) and 2 (right)

4.1.2.2 Joint 6 stations

4.1.2.2.1 Synthetic data and model

The synthetic models are matrices [100 100 1,000 1,000 10,000 10,000], [500 500 5,000 5,000 50,000 50,000], [300 300 3,000 3,000 30,000 30,000], [400 400 4,000 4,000 40,000 40,000], [150 150 3,250 3,250 25,000 25,000], and [900 900 8,000 8,000 35,000 35,000], all of the models' stations have the same thickness matrices as [20 20 50 50 80] meters and the same electrode spacing which is shown in Figure 4.17.

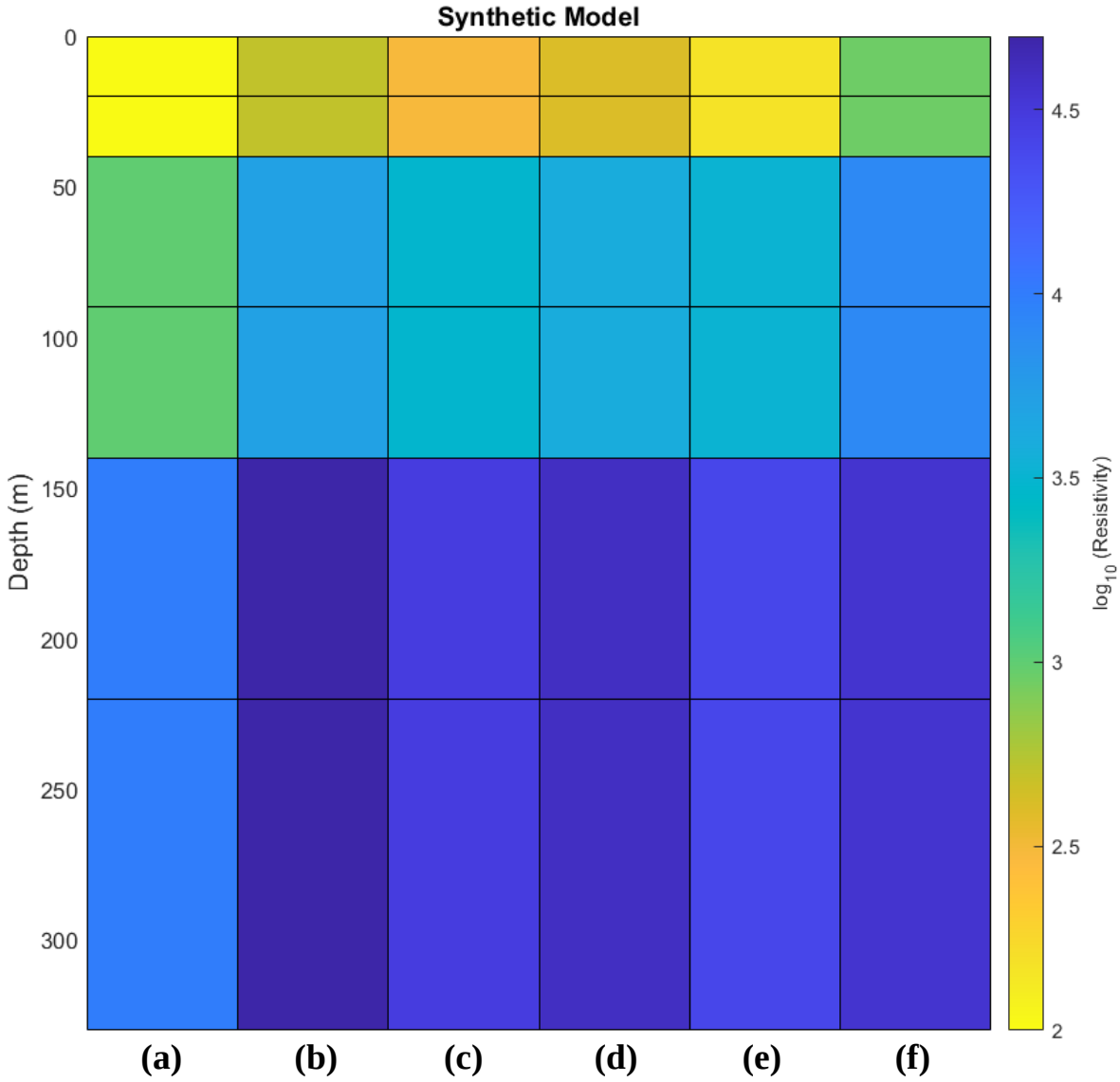

Figure 4.17 : Synthetic model of synthetic 2 layers case joint with station 1 (a), 2 (b), 3 (c), 4 (d), 5 (e) and 6 (f)

4.1.2.2.2 Inversion result

Figure 4.18 shows the apparent resistivity transform VS electrode spacing (AB/2) and mean relative error from synthetic data and calculated data which update from the initial response of synthetic data in section 4.1.2.2.1.

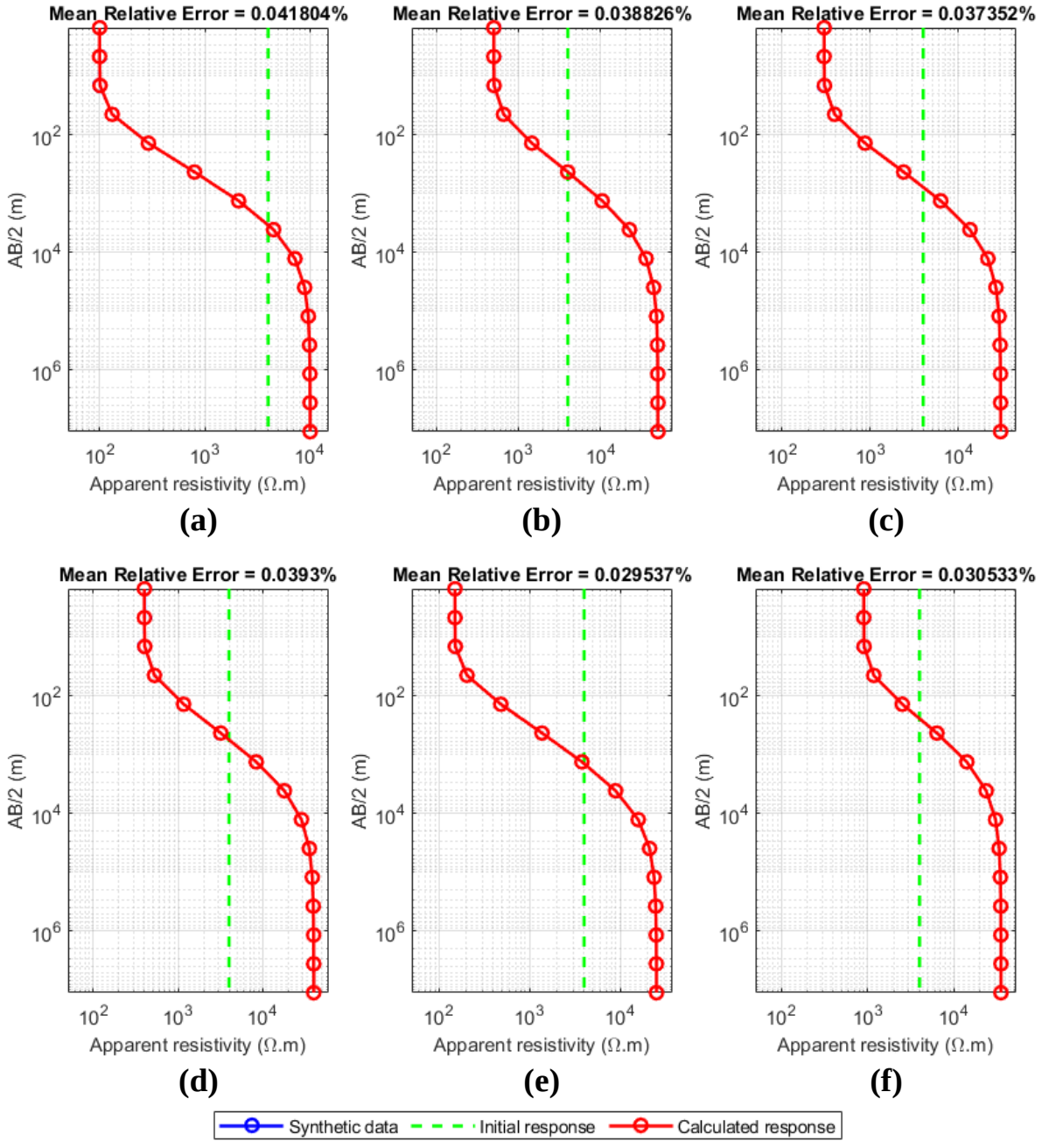

Figure 4.18 : Resistivity transform of synthetic 6 layers case joint with station 1 (a), 2 (b), 3 (c), 4 (d), 5 (e) and 6 (f)

Figure 4.19 shows the resistivity model with the pseudo depth of synthetic model and calculated model which update from the initial model and the number of iterations calculation of synthetic data in section 4.1.2.2.1.

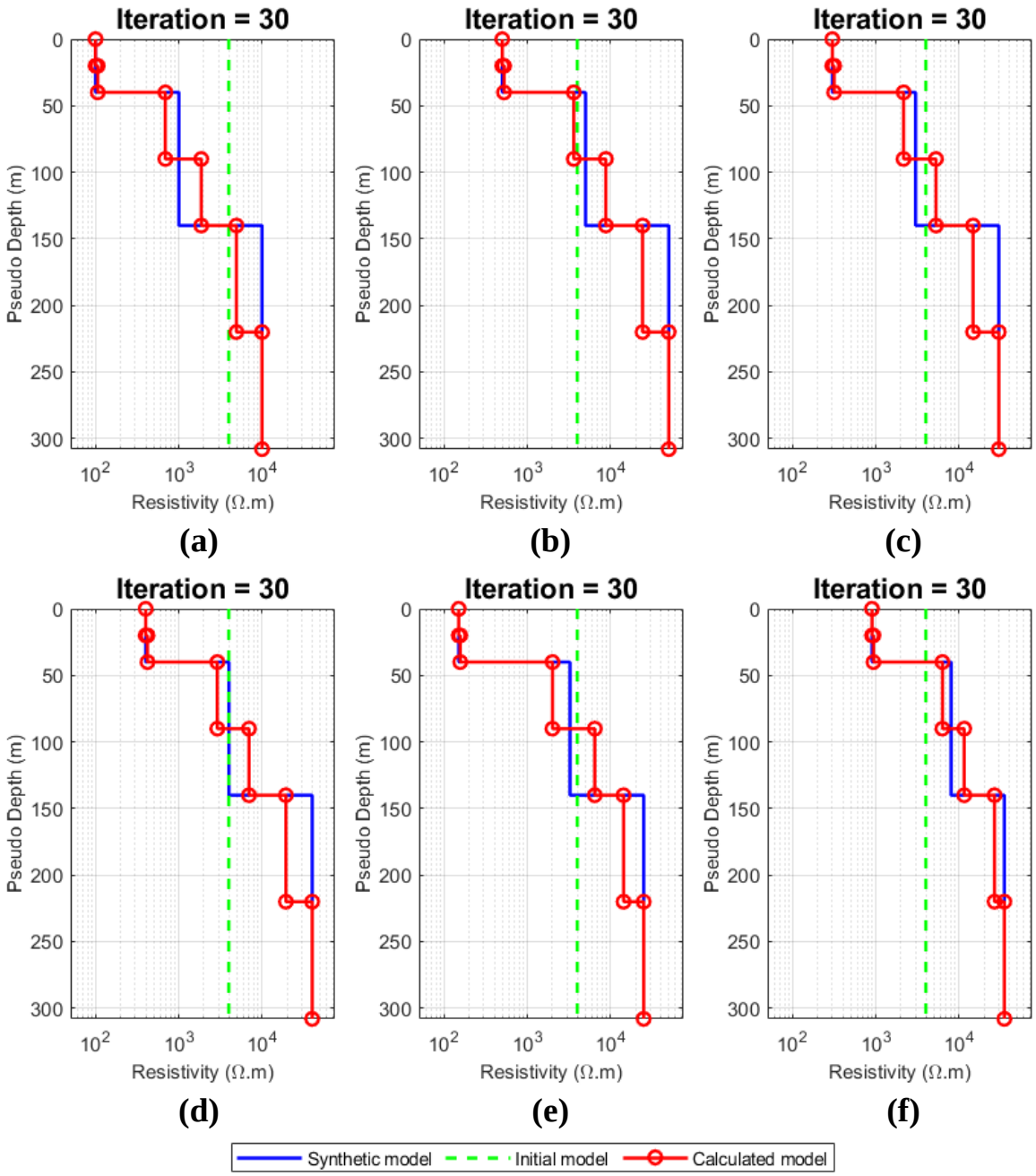

Figure 4.19 : Resistivity model of synthetic 6 layers case joint with station 1 (a), 2 (b), 3 (c), 4 (d), 5 (e) and 6 (f)

Figure 4.20 shows the calculated model which is the result from developed 1D VES program of synthetic data in section 4.1.2.2.1.

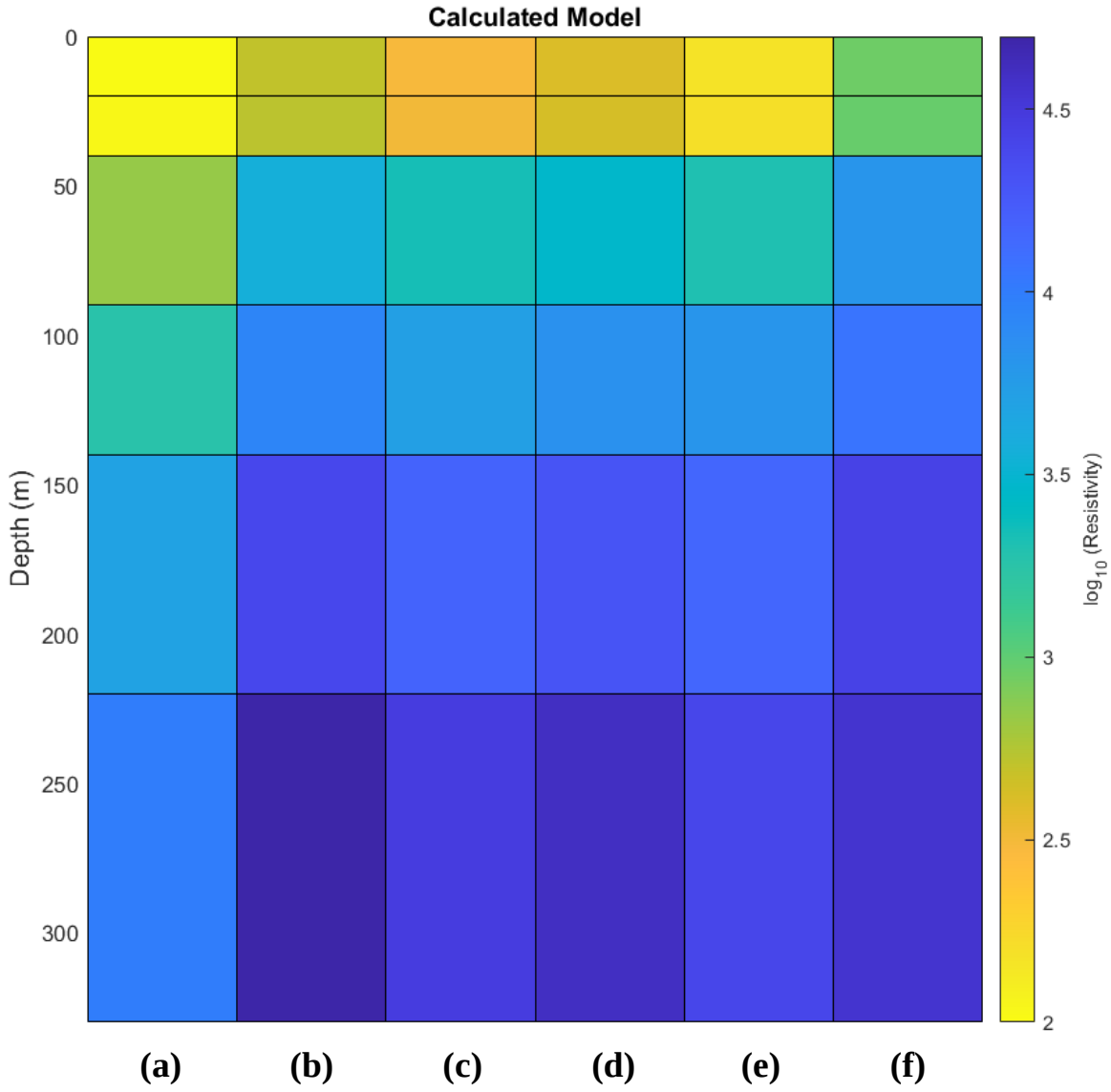

Figure 4.20 : Calculated model of synthetic 2 layers case joint with station 1 (a), 2 (b), 3 (c), 4 (d), 5 (e) and 6 (f)

4.1.2.3 Joint 9 stations

4.1.2.3.1 Synthetic data and model

The synthetic models are matrices [100 100 1,000 1,000 10,000 10,000], [500 500 5,000 5,000 50,000 50,000], [300 300 3,000 3,000 30,000 30,000], [400 400 4,000 4,000 40,000 40,000], [150 150 3,250 3,250 25,000 25,000], [900 900 8,000 8,000 35,000 35,000], [750 750 6,000 6,000 40,000 40,000], [520 520 6,500 6,500 30,000 30,000], and [210 210 4,300 4,300 26,000 26,000], all of the models' stations have the same thickness matrices as [20 20 50 50 80] meters and the same electrode spacing which is shown in Figure 4.21.

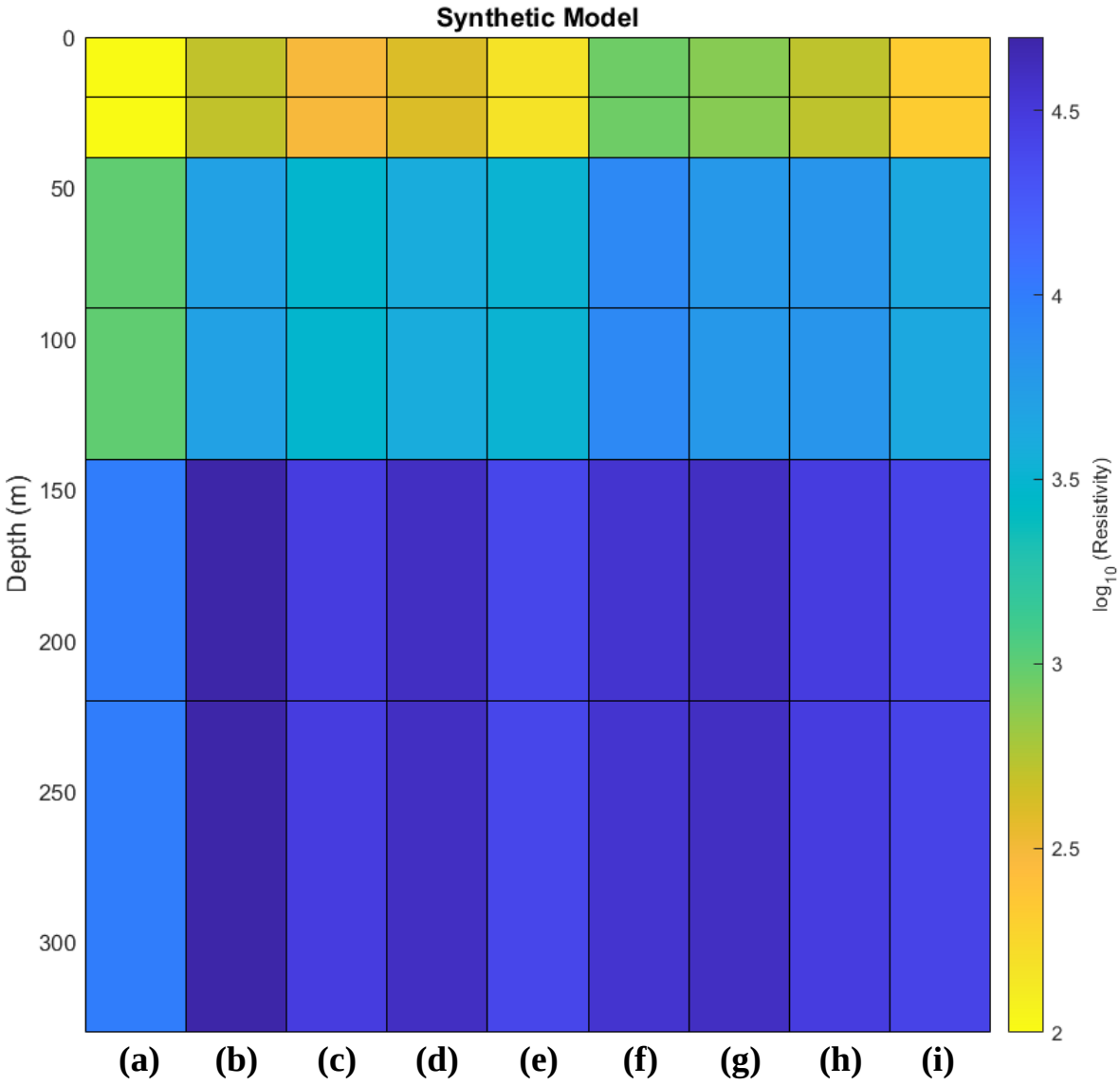

Figure 4.21 : Synthetic model of synthetic 2 layers case joint with station 1 (a), 2 (b), 3 (c), 4 (d), 5 (e), 6 (f), 7 (g), 8 (h) and 9 (i)

4.1.2.3.2 Inversion result

Figure 4.22 shows the apparent resistivity transform VS electrode spacing (AB/2) and mean relative error from synthetic data and calculated data which update from the initial response of synthetic data in section 4.1.2.3.1.

Figure 4.23 shows the resistivity model with the pseudo depth of synthetic model and calculated model which update from the initial model and the number of iterations calculation of synthetic data in section 4.1.2.3.1.

Figure 4.24 shows the calculated model which is the result from developed 1D VES program of synthetic data in section 4.1.2.3.1.

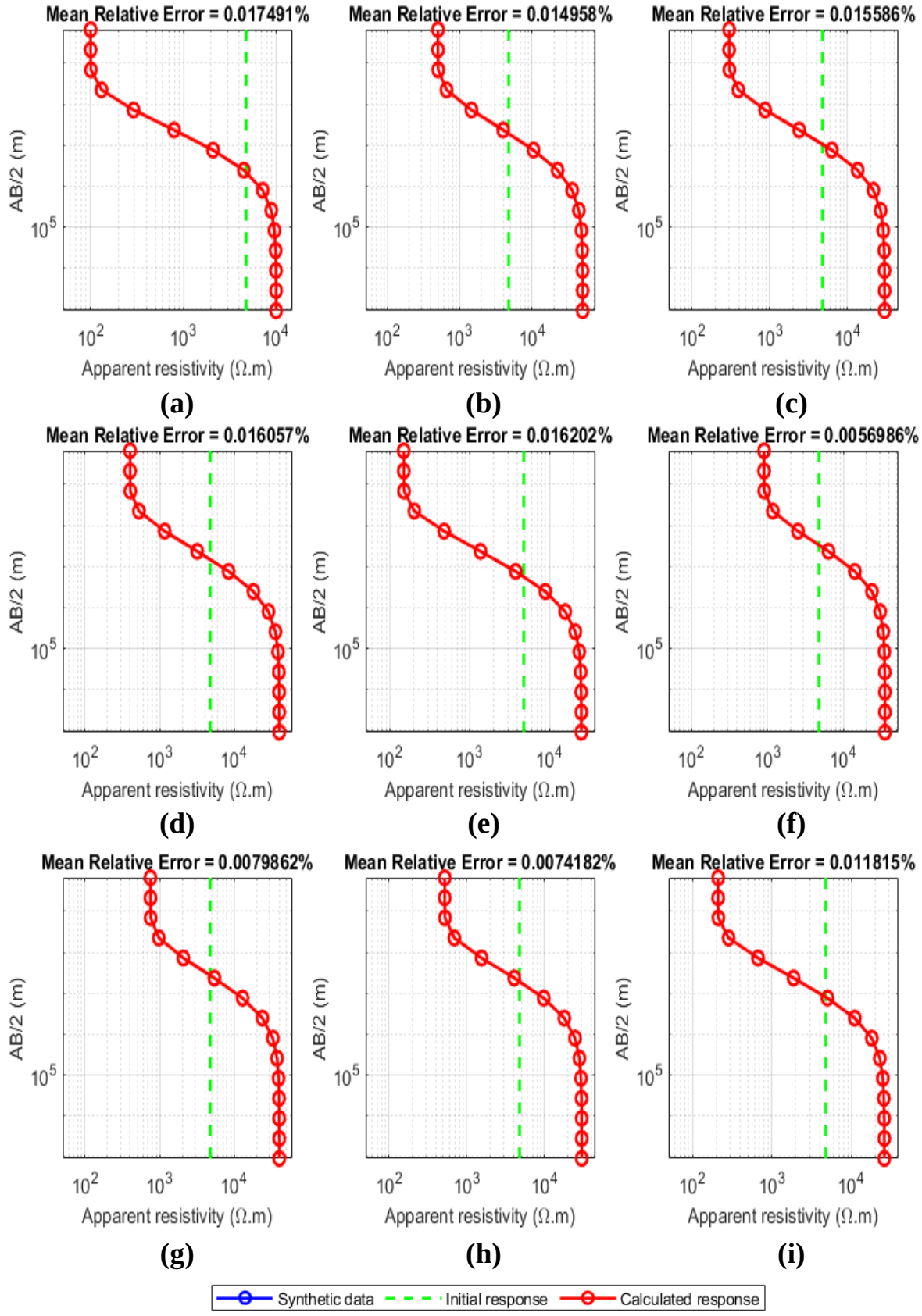

Figure 4.22 : Resistivity transform of synthetic 6 layers case joint with station 1 (a), 2 (b), 3 (c), 4 (d), 5 (e), 6 (f), 7 (g), 8 (h) and 9 (i)

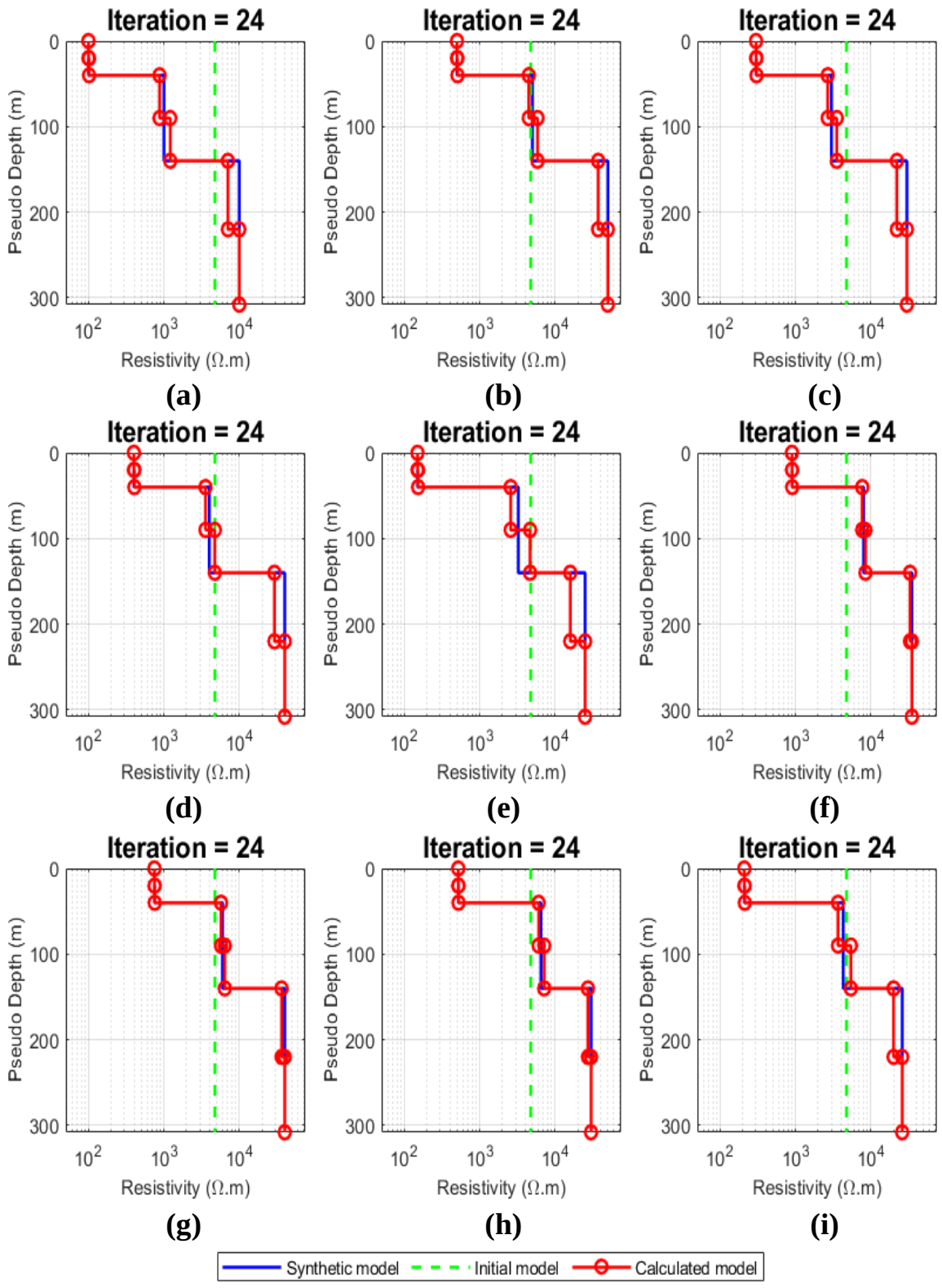

Figure 4.23 : Resistivity model of synthetic 6 layers case joint with station 1 (a), 2 (b), 3 (c), 4 (d), 5 (e), 6 (f), 7 (g), 8 (h) and 9 (i)

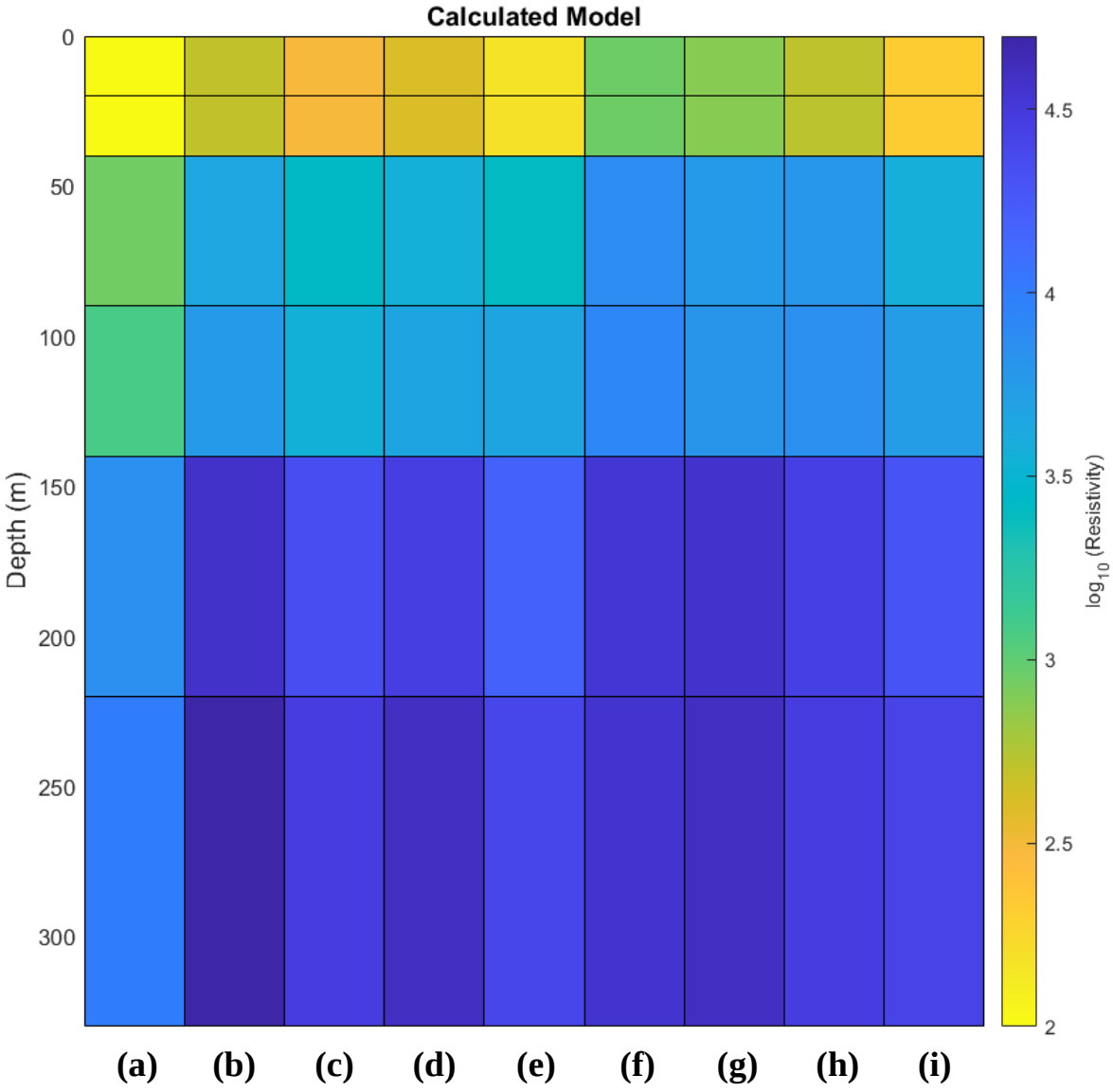

Figure 4.24 : Calculated model of synthetic 2 layers case joint with station 1 (a), 2 (b), 3 (c), 4 (d), 5 (e), 6 (f), 7 (g), 8 (h) and 9 (i)

4.1.3 Synthetic case III : 10 layers

4.1.3.1 Joint 2 stations

4.1.3.1.1 Synthetic data and model

The synthetic models are [10,000 10,000 1,000 1,000 10,000 10,000 1,000 1,000 1,000 1,000] and [15,000 15,000 1,100 1,100 13,000 13,000 1,500 1,500 5,000 5,000], both stations have the same thickness matrices as [20 20 50 50 70 70 90 90 100] meters and the same electrode spacing which is shown in Figure 4.25**.**

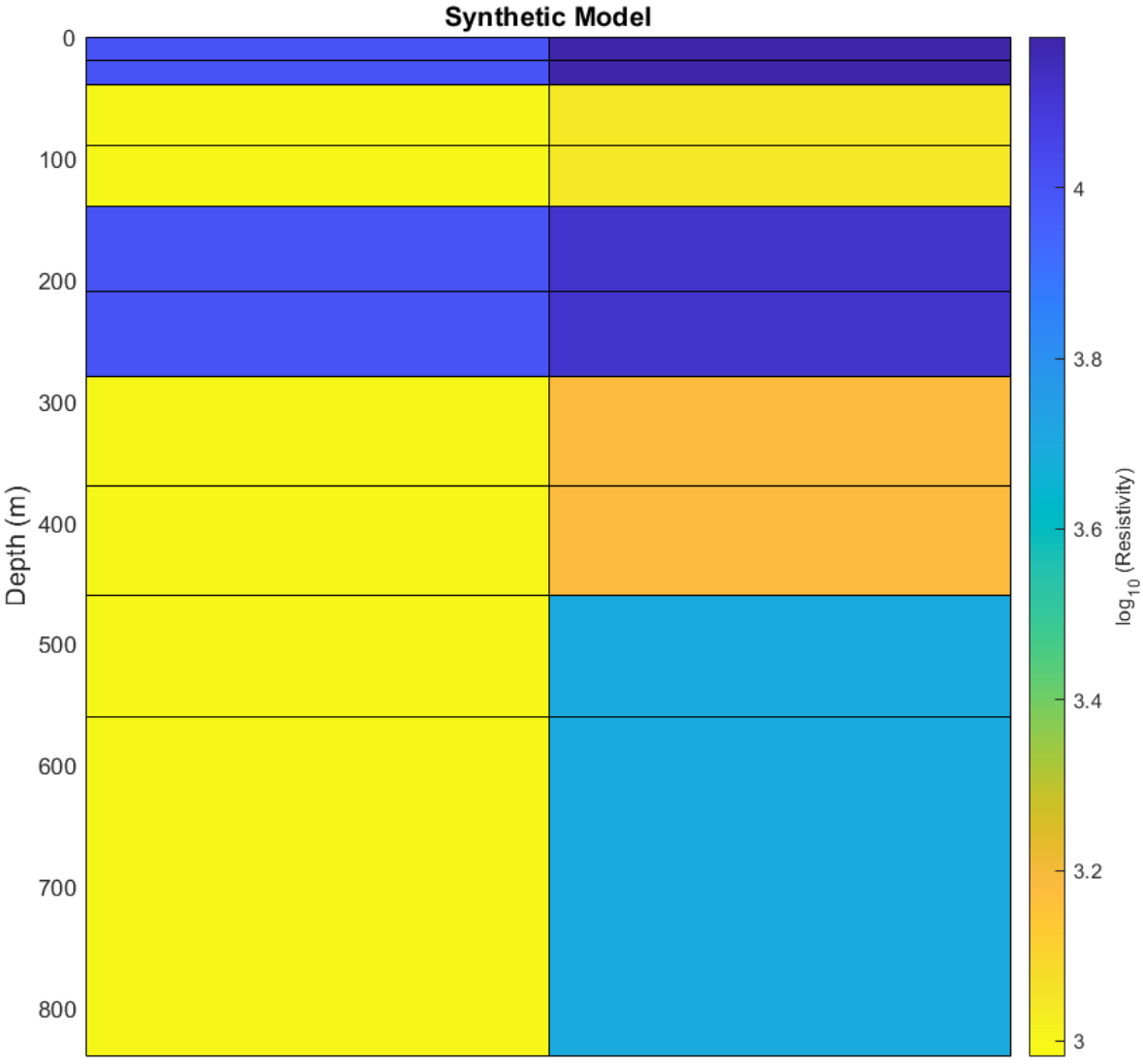

Figure 4.25 : Synthetic model of 10 layers case of station 1 (left) and 2 (right)

4.1.3.1.2 Inversion result

Figure 4.26 shows the apparent resistivity transform VS electrode spacing (AB/2) and mean relative error from synthetic data and calculated data which update from the initial response of synthetic data in section 4.1.3.1.1.

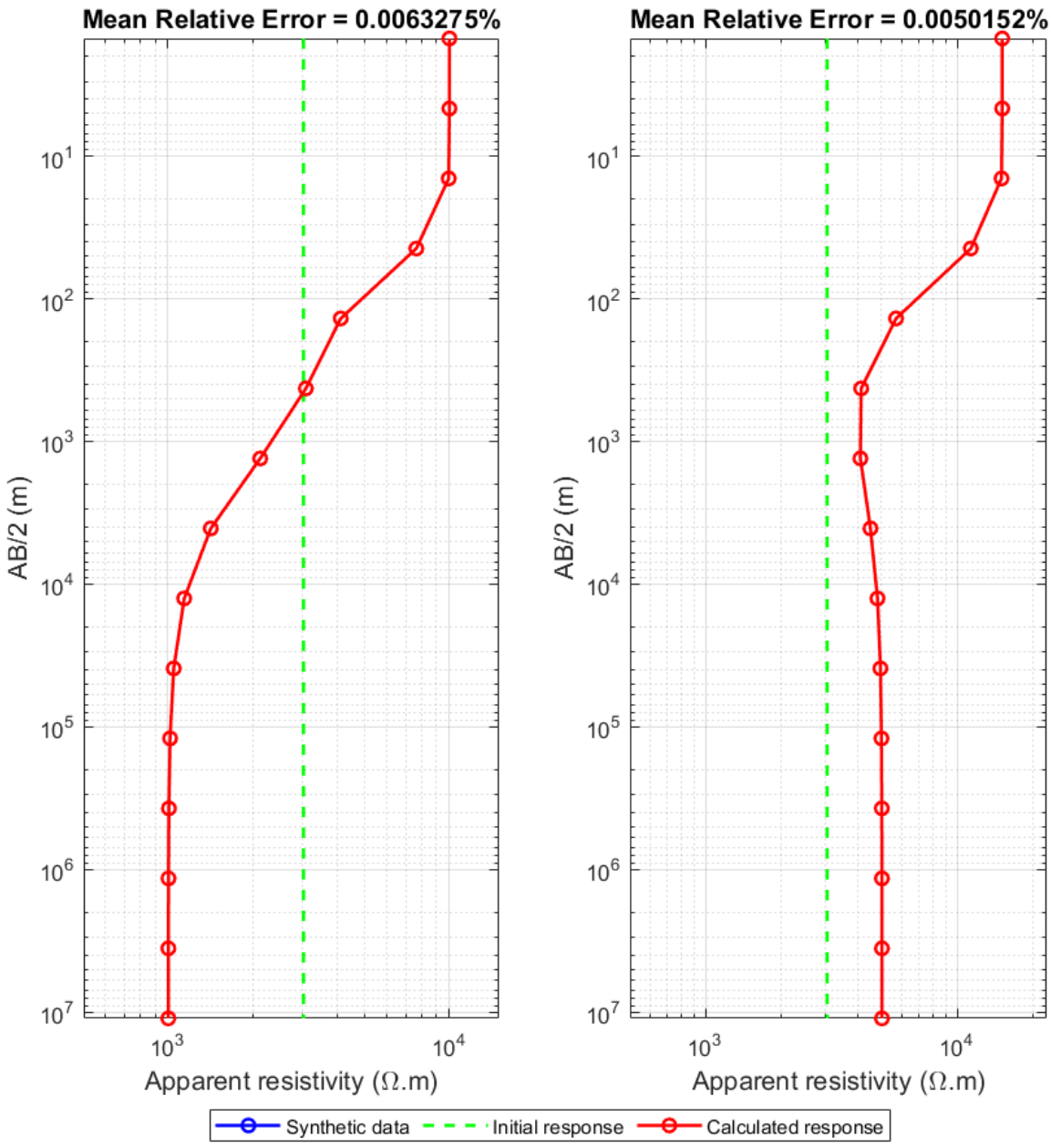

Figure 4.26 : Resistivity transform of synthetic 10 layers case joint with station 1 (left) and 2 (right)

Figure 4.27 shows the resistivity model with the pseudo depth of synthetic model and calculated model which update from the initial model and the number of iterations calculation of synthetic data in section 4.1.3.1.1.

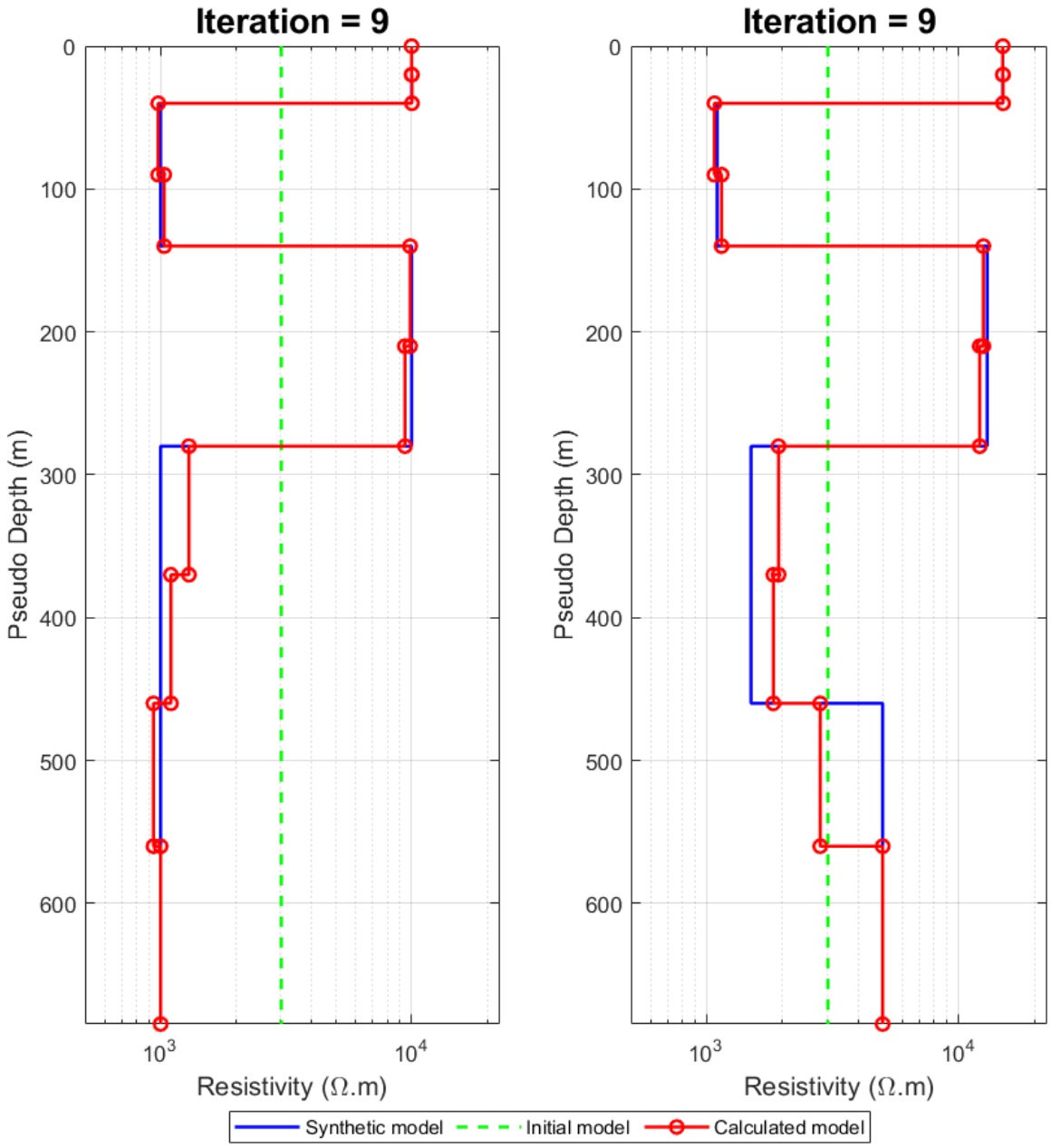

Figure 4.27 : Resistivity model of synthetic 10 layers case joint with station 1 (left) and 2 (right)

Figure 4.28 shows the calculated model which is the result from developed 1D VES program of synthetic data in section 4.1.3.1.1.

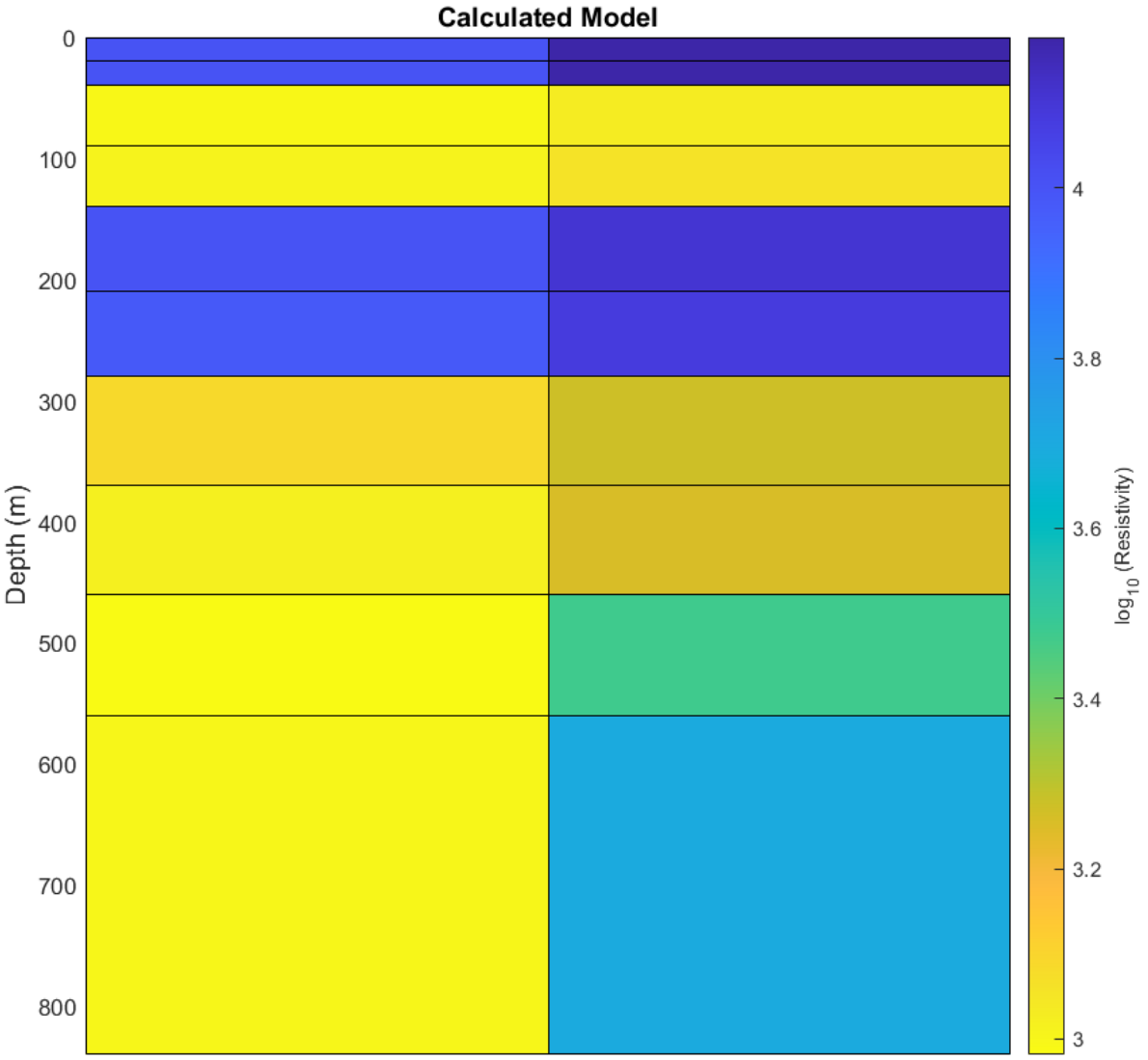

Figure 4.28 : Calculated model of 10 layers case of station 1 (left) and 2 (right)

4.1.3.2 Joint 6 stations

4.1.3.2.1 Synthetic data and model

The synthetic models are [10,000 10,000 1,000 1,000 10,000 10,000 1,000 1,000 1,000 1,000], [15,000 15,000 1,100 1,100 13,000 13,000 1,500 1,500 5,000 5,000], [13,000 13,000 1,800 1,800 20,000 20,000 1,800 1,800 2,000 2,000], [20,000 20,000 2,000 2,000 16,000 16,000 1,700 1,700 2,000 2,000], [16,500 16,500 1,550 1,550 13,700 13,700 1,700 1,700 4,500 4,500], and [12,000 12,000 1,300 1,300 14,000 14,000 1,900 1,900 3,000 3,000], all of the models' stations have the same thickness matrices as [20 20 50 50 70 70 90 90 100] meters and the same electrode spacing which is shown in Figure 4.29.

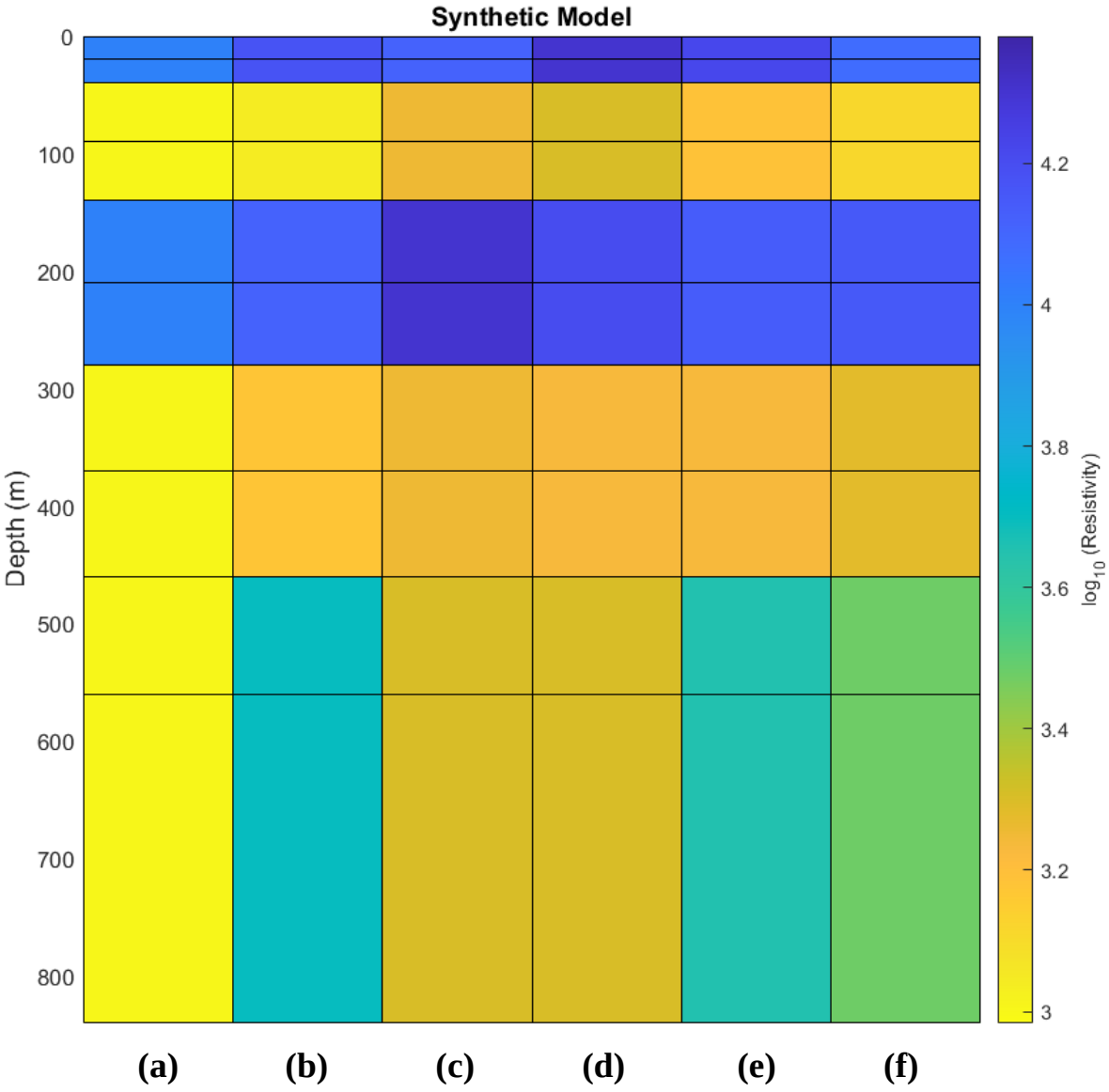

Figure 4.29 : Synthetic model of synthetic 2 layers case joint with station 1 (a), 2 (b), 3 (c), 4 (d), 5 (e) and 6 (f)

4.1.3.2.2 Inversion result

Figure 4.30 shows the apparent resistivity transform VS electrode spacing (AB/2) and mean relative error from synthetic data and calculated data which update from the initial response of synthetic data in section 4.1.3.2.1.

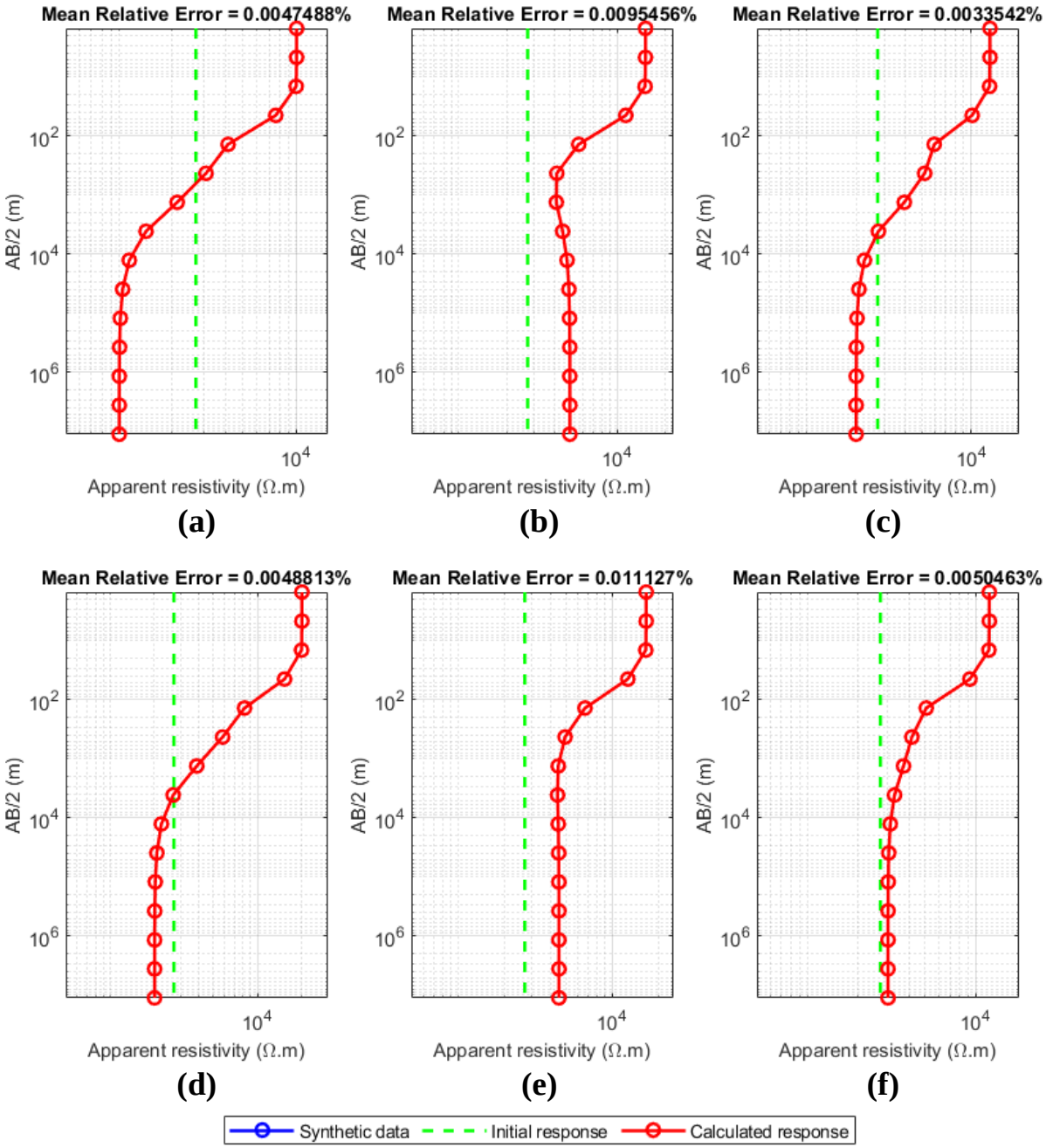

Figure 4.30 : Resistivity transform of synthetic 10 layers case joint with station 1 (a), 2 (b), 3 (c), 4 (d), 5 (e) and 6 (f)

Figure 4.31 shows the resistivity model with the pseudo depth of synthetic model and calculated model which update from the initial model and the number of iterations calculation of synthetic data in section 4.1.3.2.1.

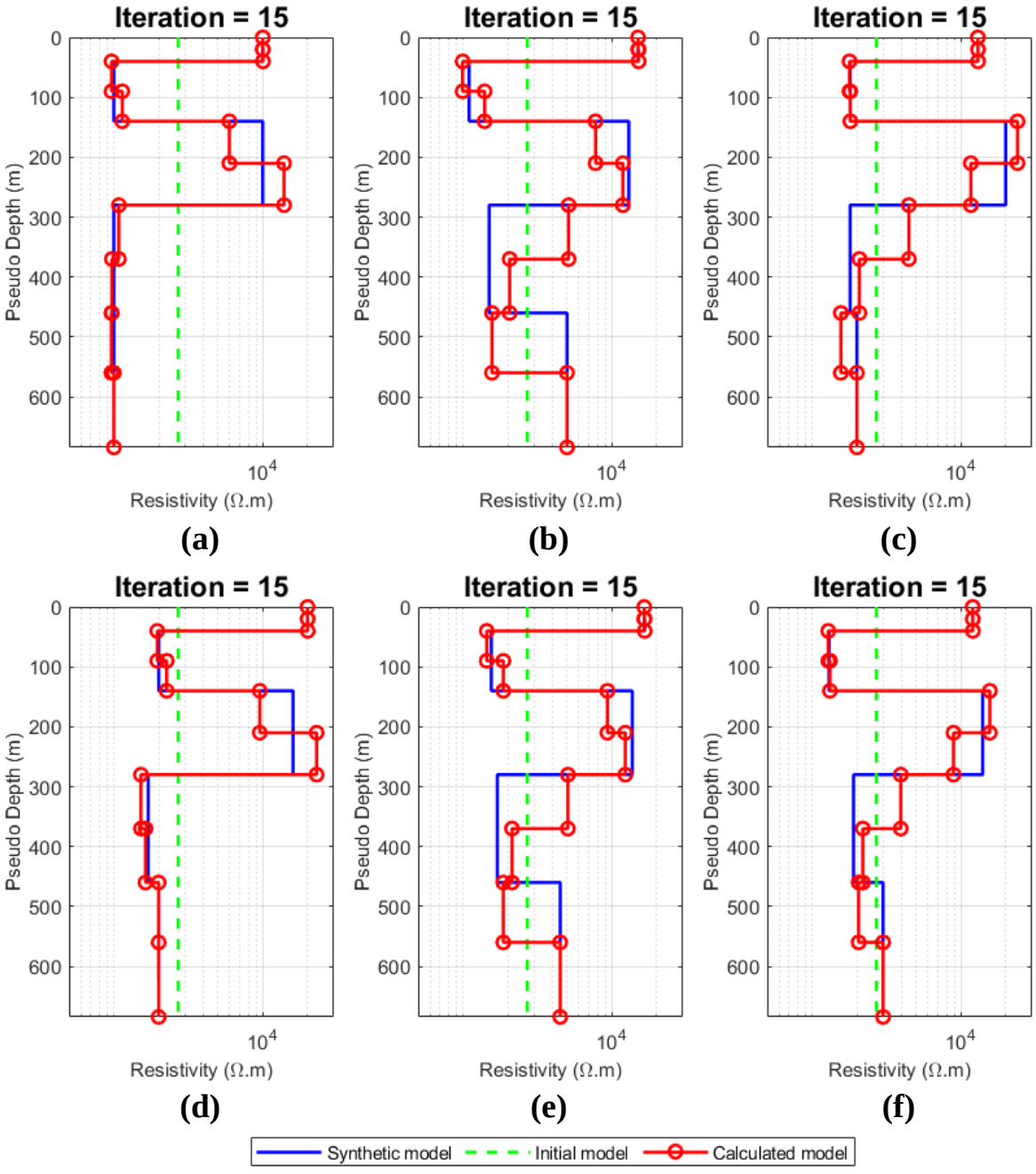

Figure 4.31 : Resistivity model of synthetic 10 layers case joint with station 1 (a), 2 (b), 3 (c), 4 (d), 5 (e) and 6 (f)

Figure 4.32 shows the calculated model which is the result from developed 1D VES program of synthetic data in section 4.1.3.2.1.

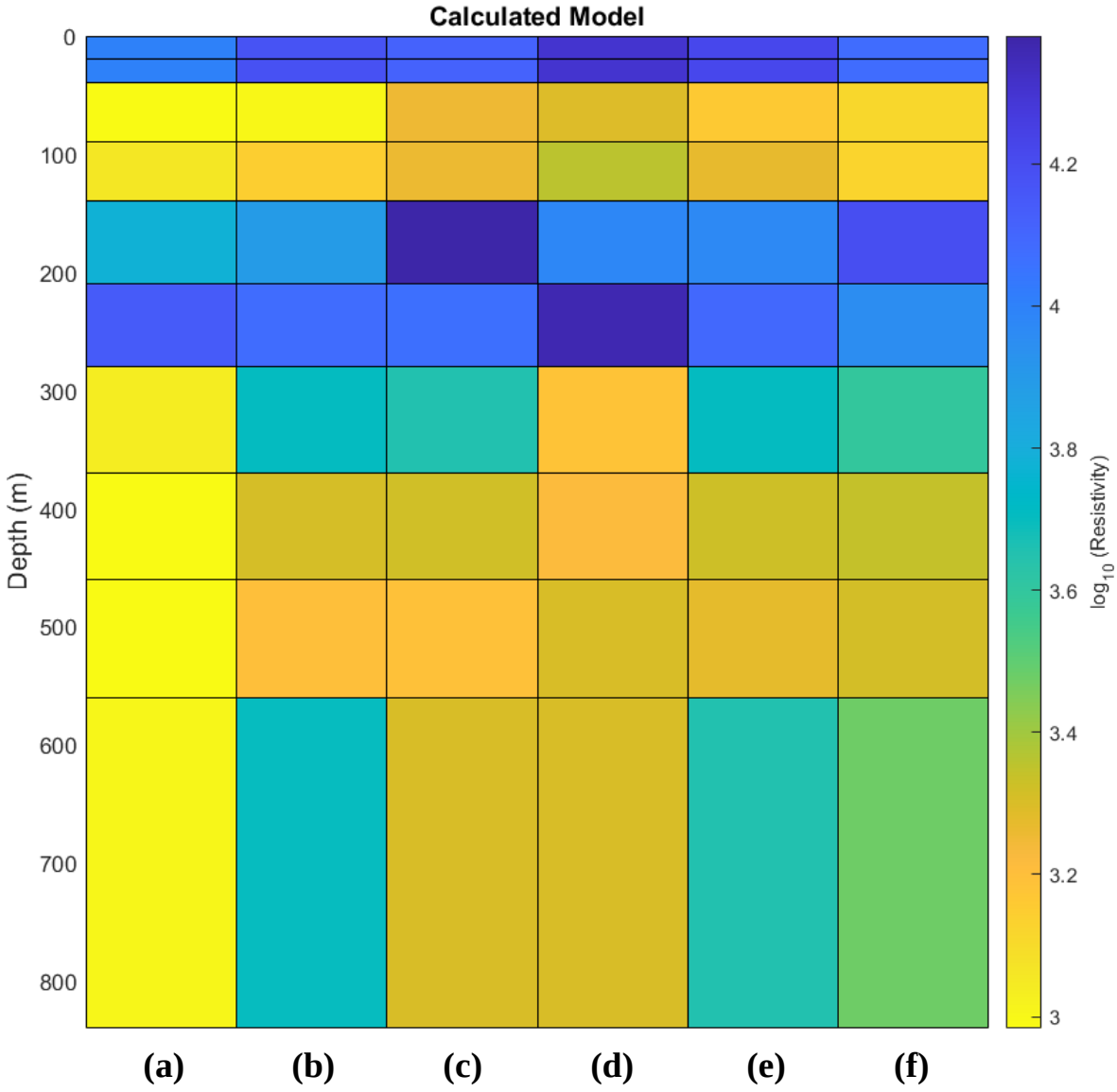

Figure 4.32 : Calculated model of synthetic 2 layers case joint with station 1 (a), 2 (b), 3 (c), 4 (d), 5 (e) and 6 (f)

4.1.3.3 Joint 9 stations

4.1.3.3.1 Synthetic data and model

The synthetic models are [10,000 10,000 1,000 1,000 10,000 10,000 1,000 1,000 1,000 1,000], [15,000 15,000 1,100 1,100 13,000 13,000 1,500 1,500 5,000 5,000], [13,000 13,000 1,800 1,800 20,000 20,000 1,800 1,800 2,000 2,000], [20,000 20,000 2,000 2,000 16,000 16,000 1,700 1,700 2,000 2,000], [16,500 16,500 1,550 1,550 13,700 13,700 1,700 1,700 4,500 4,500], [12,000 12,000 1,300 1,300 14,000 14,000 1,900 1,900 3,000 3,000], [25,000 25,000 3,100 3,100 23,000 23,000 2,500 2,500 3,000 3,000], [19,500 19,500 1,150 1,150 11,500 11,500 1,900 1,900 2,550 2,550], and [21,000 21,000 2,100 2,100 23,000 23,000 1,800 1,800 4,500 4,500], all of the models' stations have the same thickness matrices as [20 20 50 50 70 70 90 90 100] meters and the same electrode spacing which is shown in Figure 4.33.

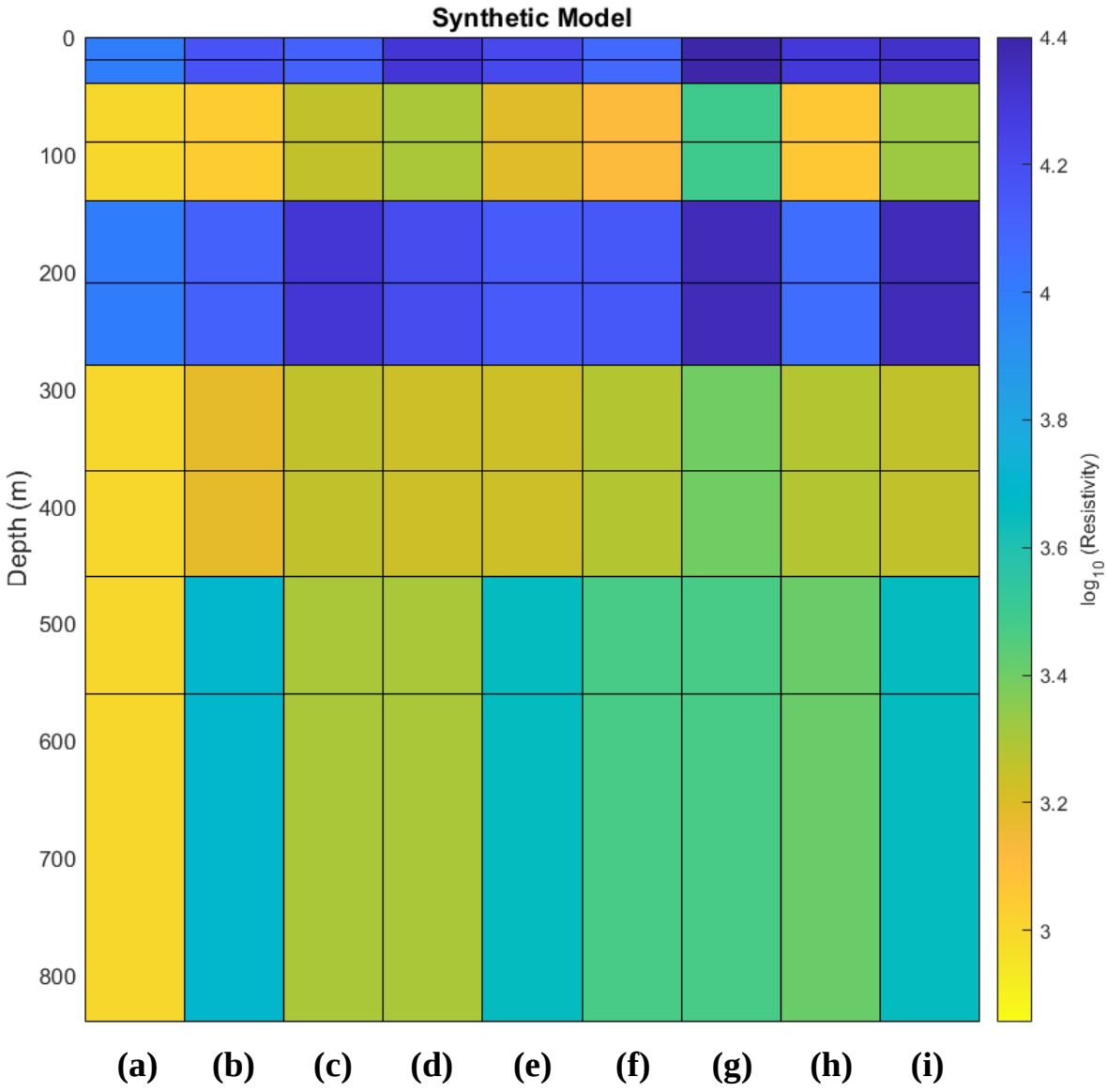

Figure 4.33 : Synthetic model of synthetic 2 layers casejoint with station 1 (a), 2 (b), 3 (c), 4 (d), 5 (e), 6 (f), 7 (g), 8 (h) and 9 (i)

4.1.3.3.2 Inversion result

Figure 4.34 shows the apparent resistivity transform VS electrode spacing (AB/2) and mean relative error from synthetic data and calculated data which update from the initial response of synthetic data in section 4.1.3.3.1.

Figure 4.35 shows the resistivity model with the pseudo depth of synthetic model and calculated model which update from the initial model and the number of iterations calculation of synthetic data in section 4.1.3.3.1.

Figure 4.36 shows the calculated model which is the result from developed 1D VES program of synthetic data in section 4.1.3.3.1.

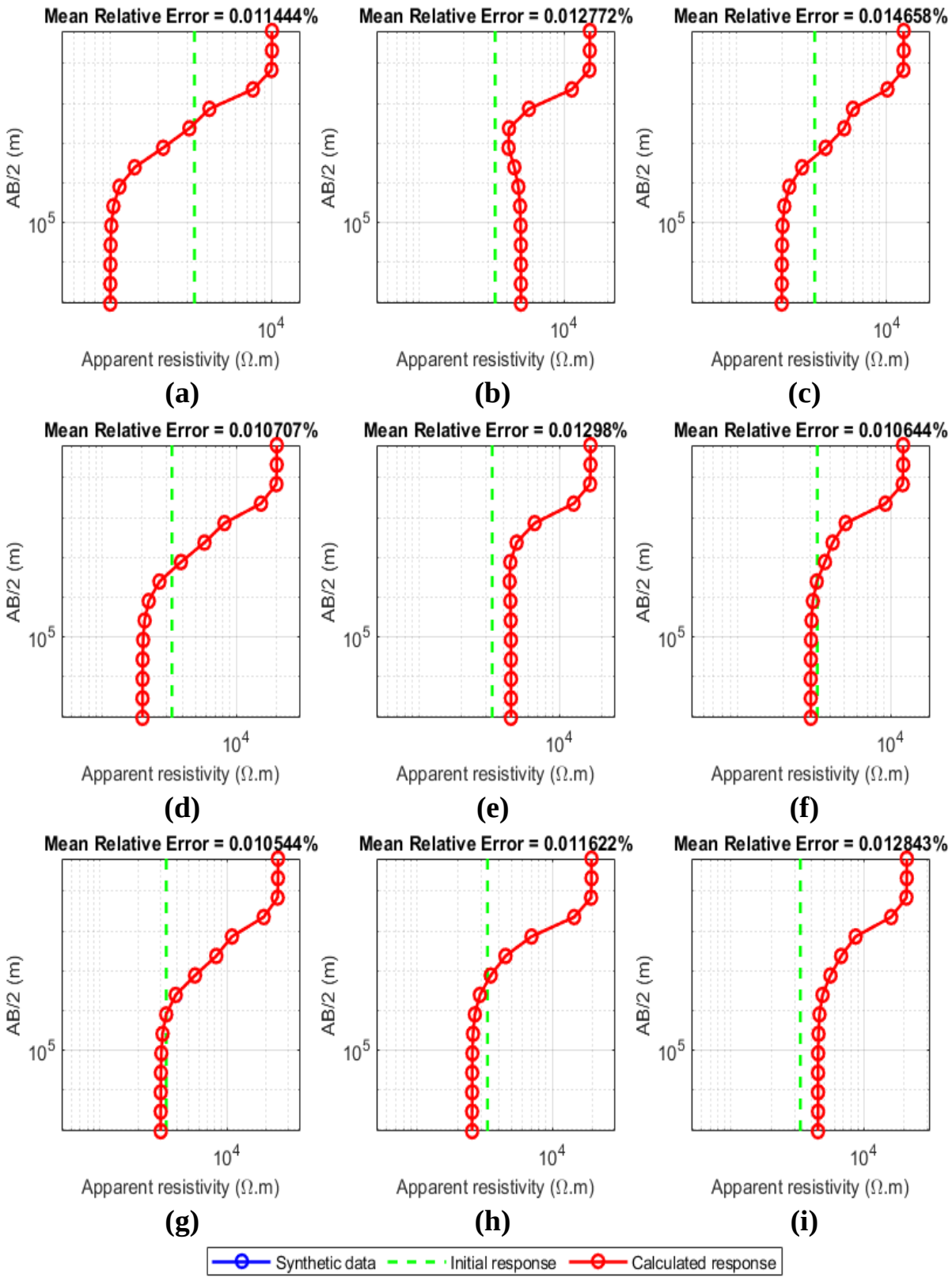

Figure 4.34 : Resistivity transform of synthetic 6 layers case joint with station 1 (a), 2 (b), 3 (c), 4 (d), 5 (e), 6 (f), 7 (g), 8 (h) and 9 (i)

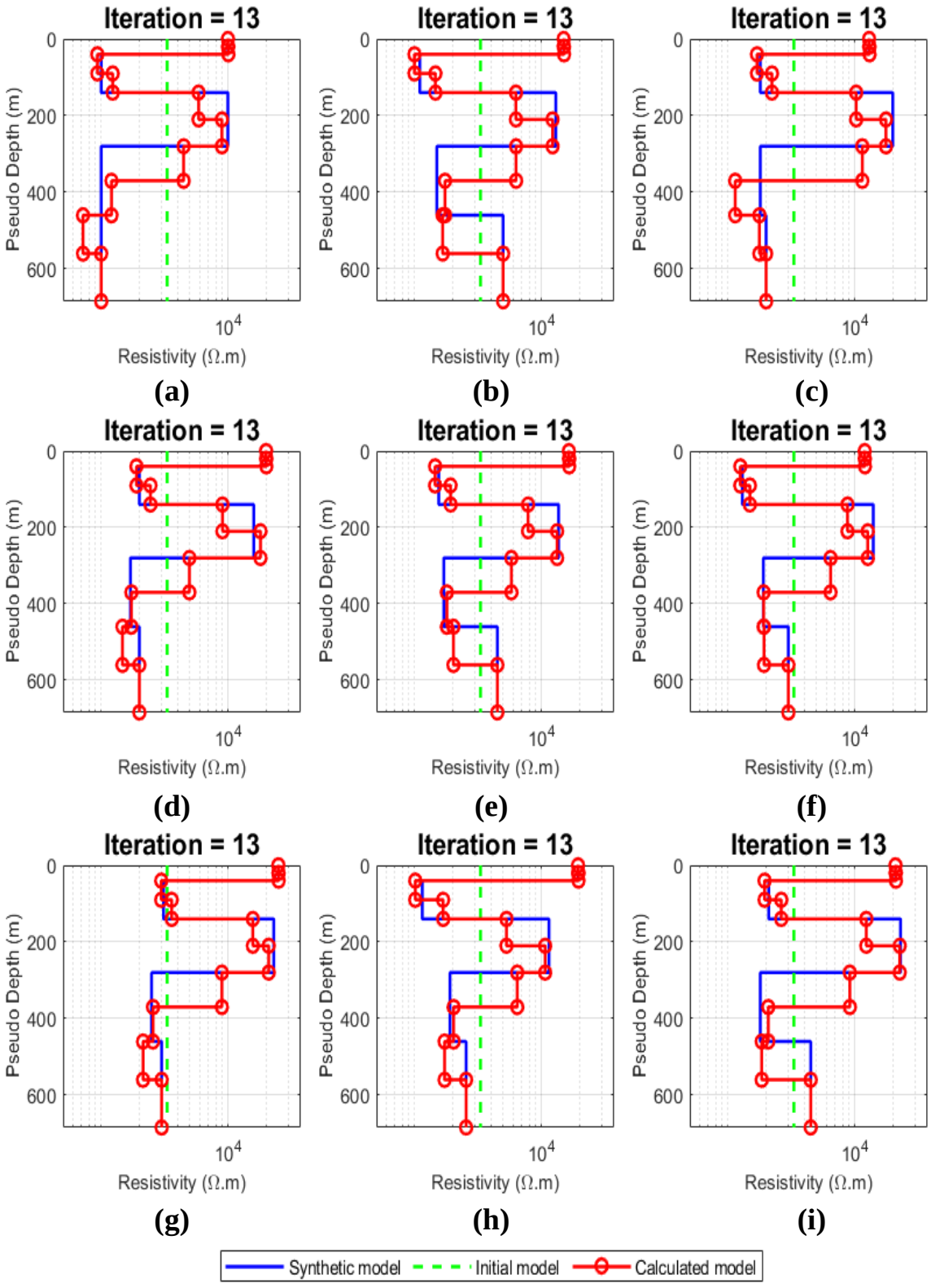

Figure 4.35 : Resistivity model of synthetic 6 layers case joint with station 1 (a), 2 (b), 3 (c), 4 (d), 5 (e), 6 (f), 7 (g), 8 (h) and 9 (i)

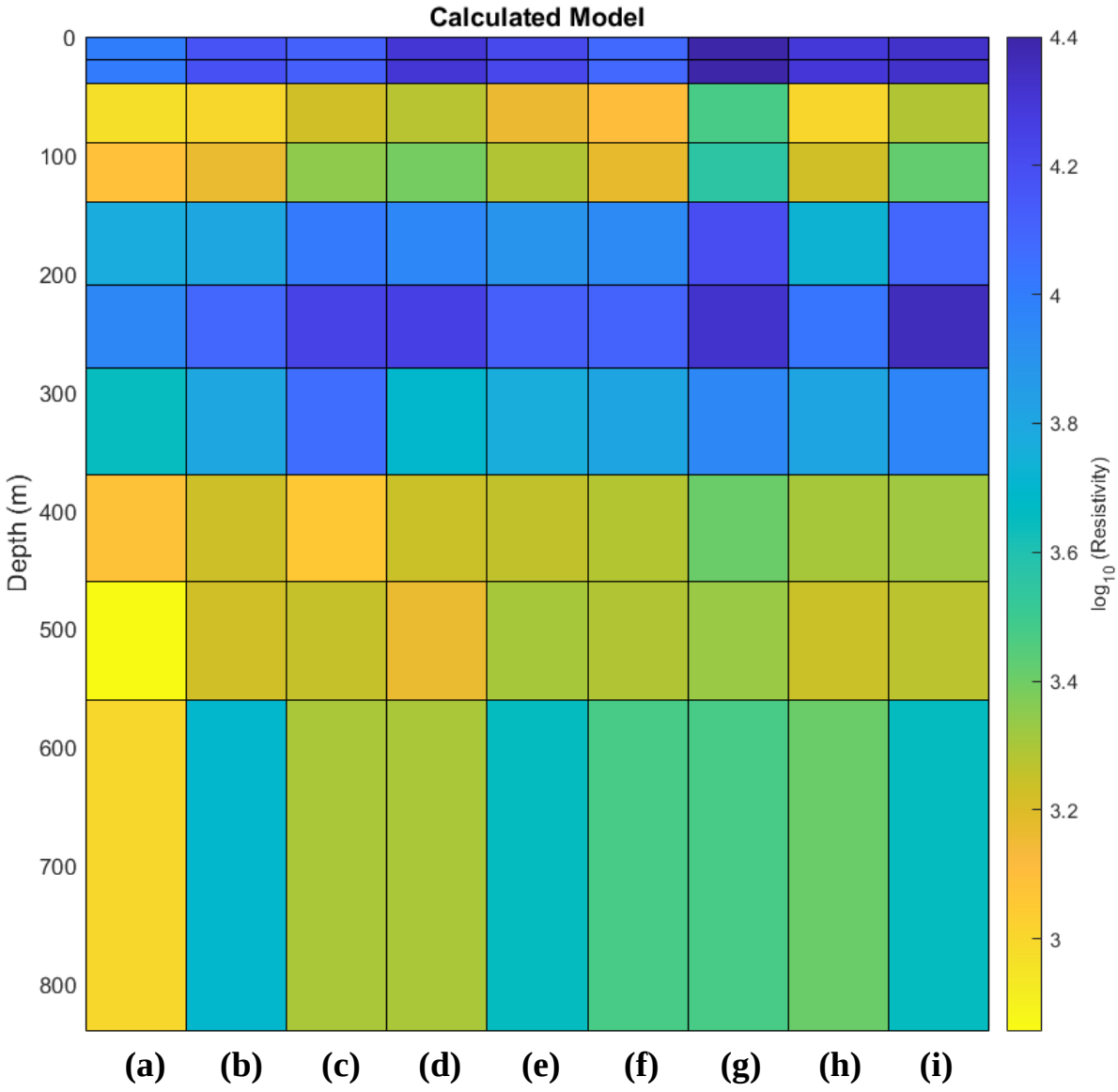

Figure 4.36 : Calculated model of synthetic 2 layers casejoint with station 1 (a), 2 (b), 3 (c), 4 (d), 5 (e), 6 (f), 7 (g), 8 (h) and 9 (i)

4.2 Real Experiment

In this section will show the applicability of code by applying the code to the real observed data from Dr. Puwis Amatyakul. The study area is located in Sai Yok, Kanchanaburi, Thailand. The goal of the surveys is to map the resistivity structure to study the fault zone.

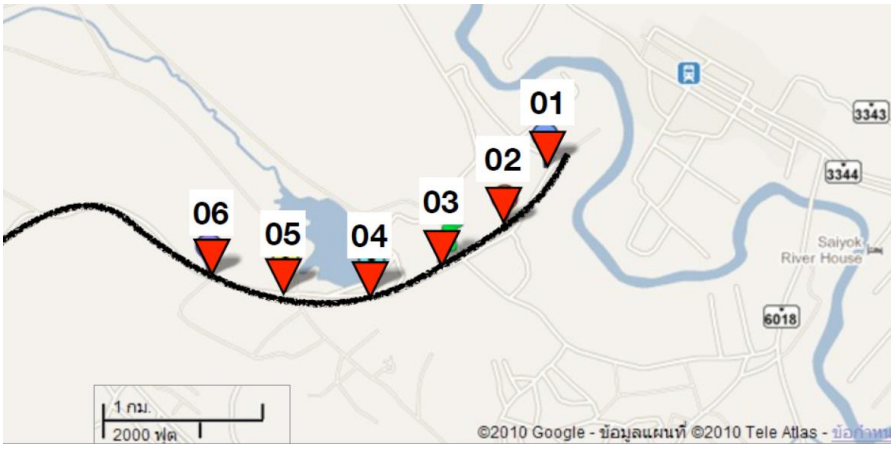

Figure 4.37 : The study area at Sai Yok, Kanchanaburi, Thailand. The established survey is used Schlumberger VES surveys. (cite : Dr.Puwis Amatyakul, 2010)

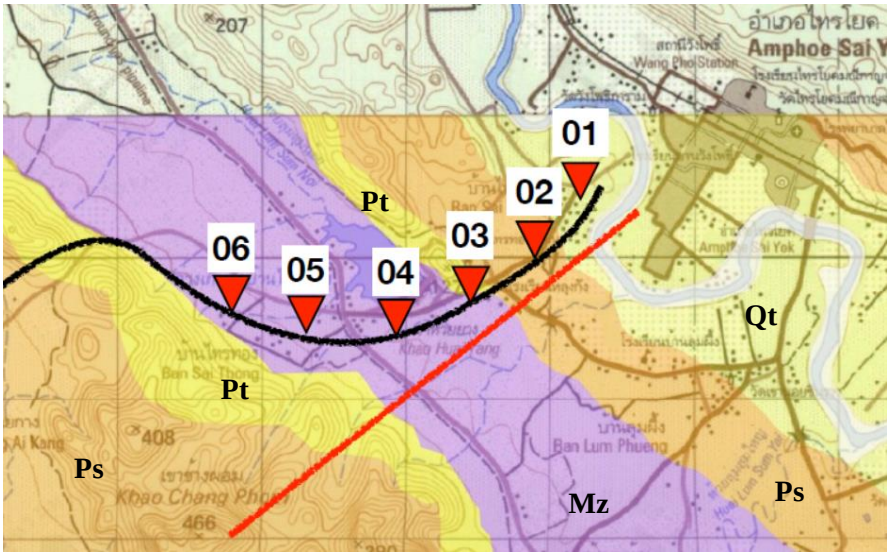

Figure 4.38 : The geological map from the study area. Mz is sandstone type I, Pt is sandstone type II, Ps is limestone, Qt is sedimentary rock (cite : Dr.Puwis Amatyakul, 2010)

4.2.1 Inversion result

Figure 4.39 shows the apparent resistivity transform VS electrode spacing (AB/2) and mean relative error from real data and calculated data which update from the initial response of observed data (cite : Dr.Puwis Amatyakul, 2010).

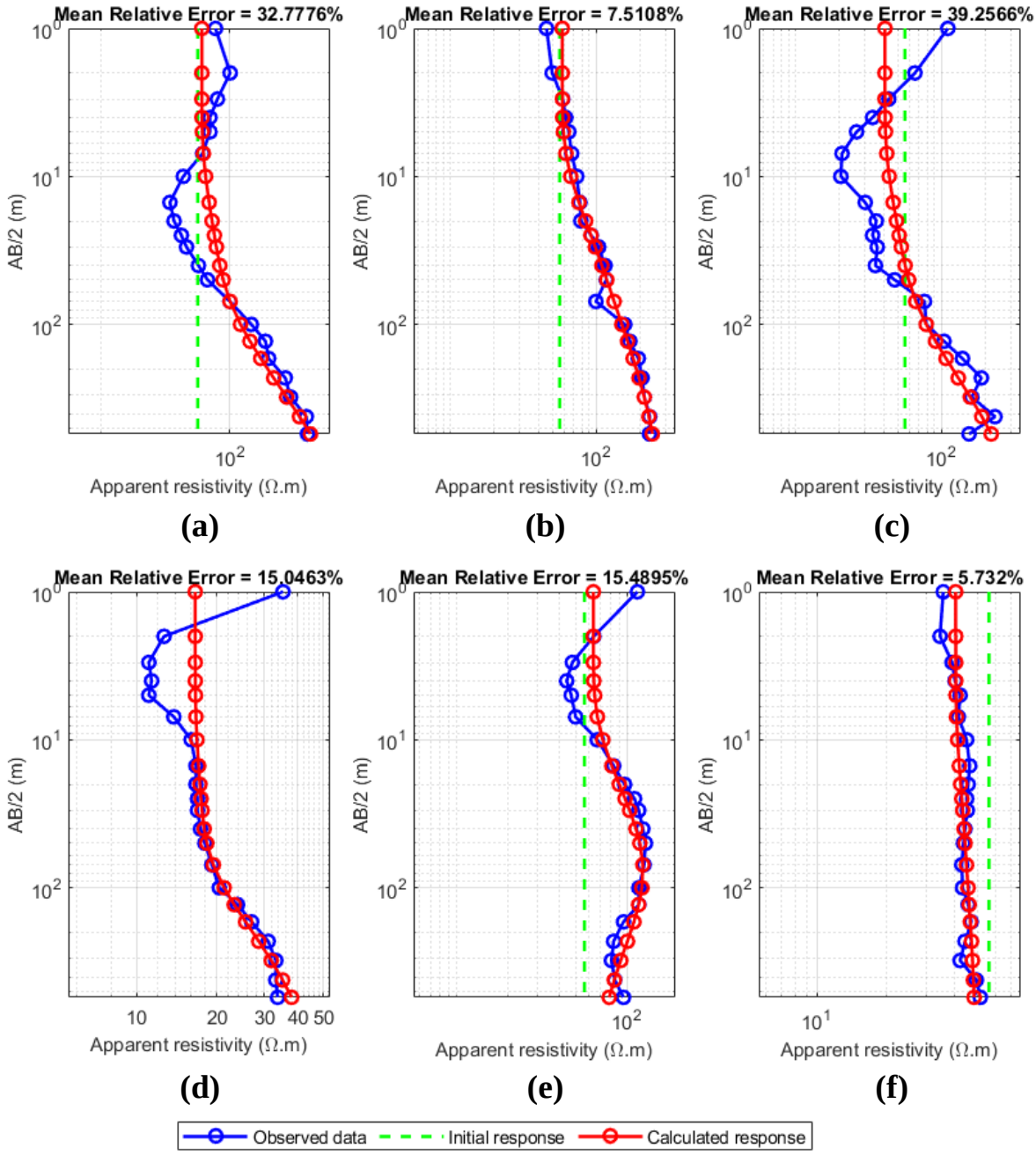

Figure 4.39 : Resistivity transform of observed data case joint with station 1 (a), 2 (b), 3 (c), 4 (d), 5 (e) and 6 (f)

Figure 4.40 shows the resistivity model with the pseudo depth of calculated model which update from the initial model and the number of iterations calculation of observed data (cite : Dr.Puwis Amatyakul, 2010).

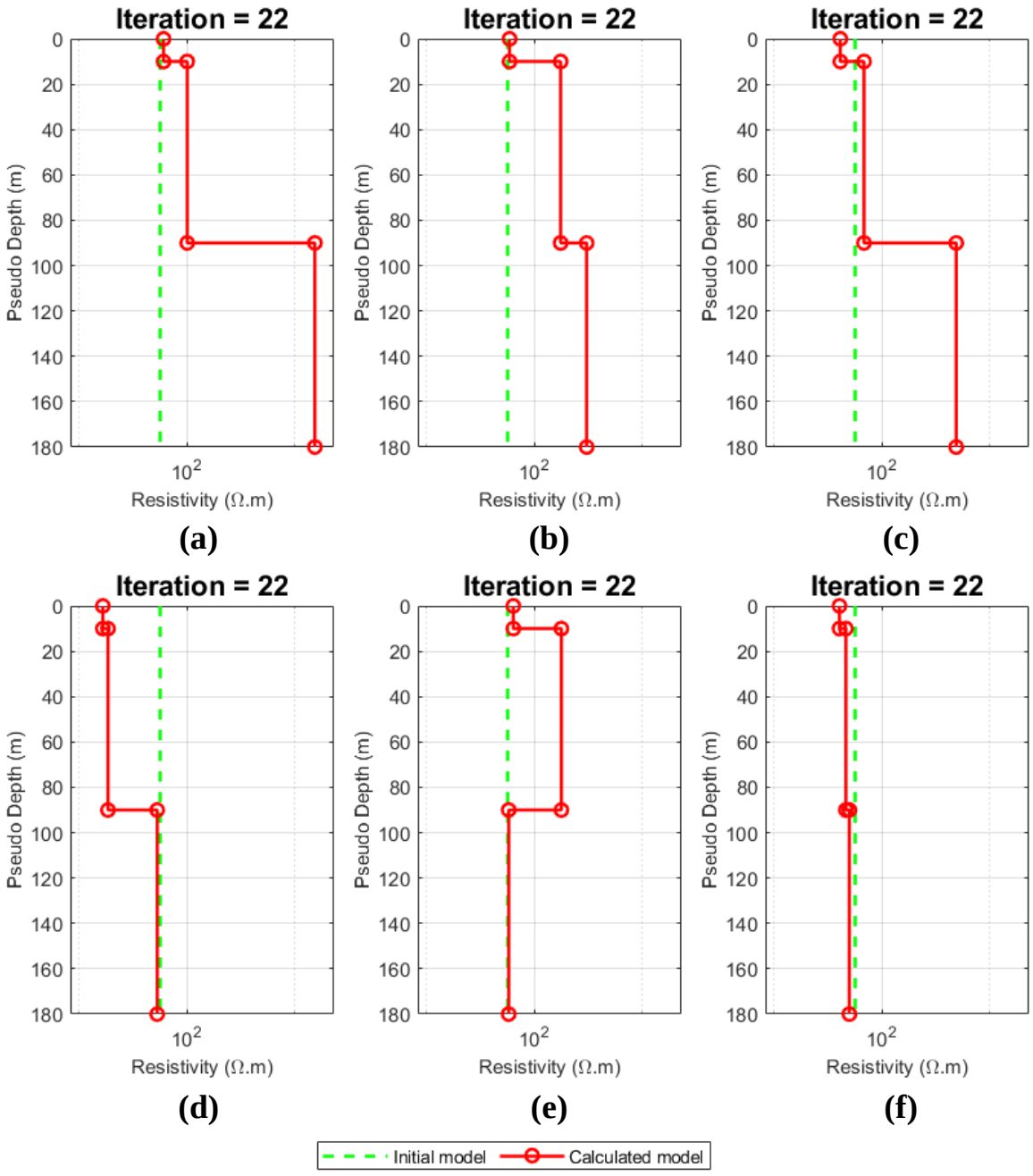

Figure 4.40 : Resistivity model of observed data case joint with station 1 (a), 2 (b), 3 (c), 4 (d), 5 (e) and 6 (f)

Figure 4.41 shows the calculated model which is the result from developed 1D VES program of observed data (cite : Dr.Puwis Amatyakul, 2010).

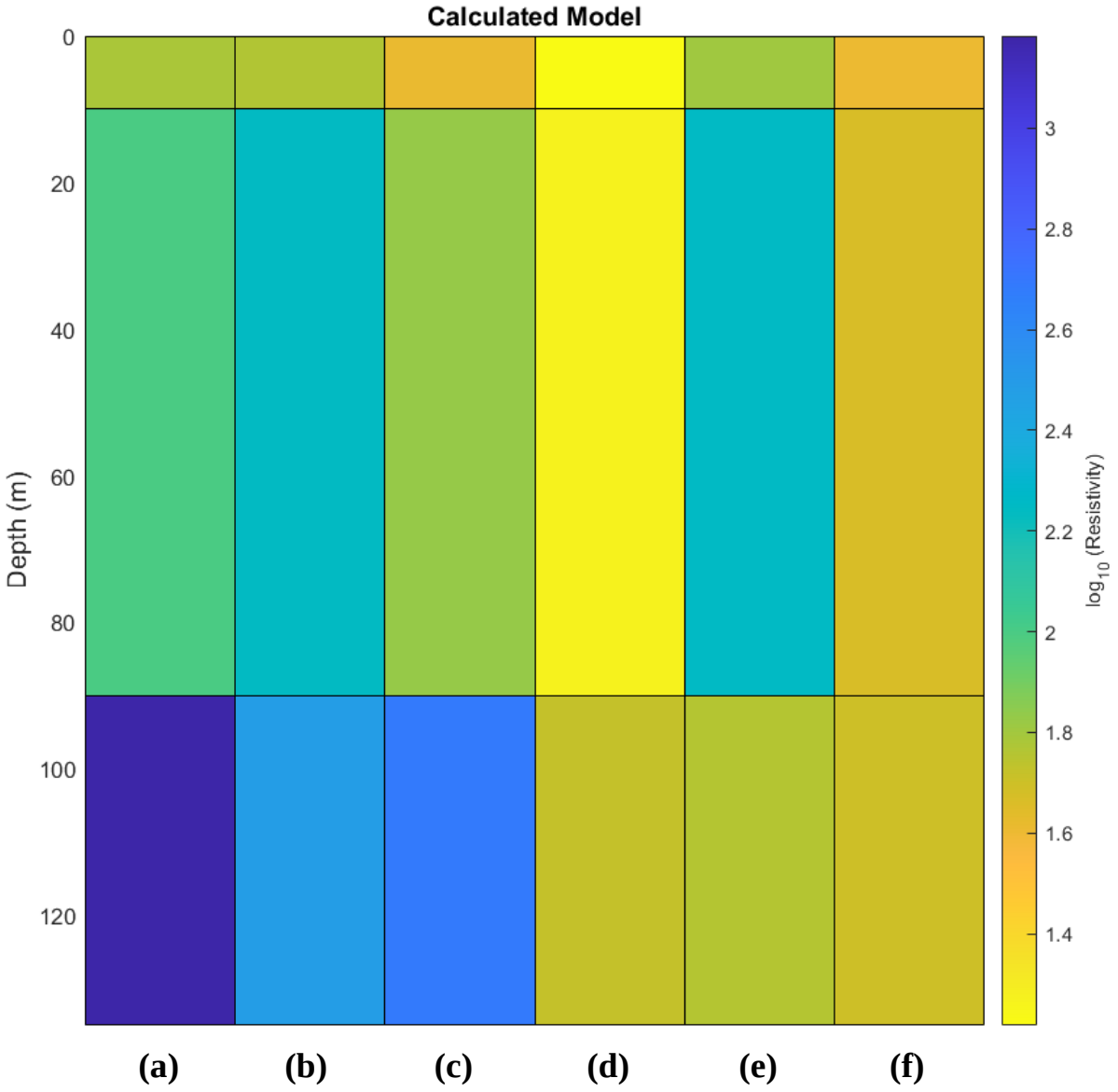

Figure 4.41 : Calculated model of observed data case joint with station 1 (a), 2 (b), 3 (c), 4 (d), 5 (e) and 6 (f)

4.3 Discussion and Conclusion

From the result, the developed 1D VES inversion code with a lateral constraint can apply the real data from vertical electrical sounding exploration from the study area at Sai Yok, Kanchanaburi, Thailand and obtain the subsurface resistivity model beneath many station sites.

The resolution and the reliability of the model obtained from the developed 1D VES inversion code are approximate to those from the individual inversion, in addition, the results of developed 1D VES inversion code were weighted by the acquired data from the nearby stations which affect to the continuity between nearby stations.

Therefore, we have verified that the developed 1D VES inversion with lateral constraint works for both synthetic tests and for the real experiment. The obtained model from the joint inversion is accurate and reliable resembles the single inversions.

Chapter 5

Summary

This research aims to create the 1D Vertical Electrical Sounding (VES) inversion with a Lateral constraint program.

In order to develop the efficient 1D VES inversion with a lateral constraint, this research follow the Occam's inversion proposed by Amatyakul (2010). Occam's inversion has the roughness operator in the inversion system that affects the continuity of the model layer both vertical and horizontal.

The developed 1D VES inversion codes are written about 300 lines of MATLAB program. All the codes can run and test with both synthetic and real experiments case. The results show that the developed 1D VES inversion code works with both synthetic and real data by can join the nearby station many stations into the calculation for helping to generate the models which have the continuity between layer and stations.

The research validates the developed code with the synthetic experiment. The synthetic case shows that the developed code is working for joint the nearby station many stations in co-calculation.

The results from both synthetic and real experiments demonstrate that the obtained models from developed 1D VES inversion code approximate to those from the individual inversion. In addition, the results have the continuity that supports and reduce the time for comparing and selecting the inversion's results from many stations.

Although the resolution and reliability of the results obtained from the developed 1D VES inversion code of this research are inferior to another inversion program which was used and calculated in industrial and real geophysics exploration, the developed 1D VES inversion code of this research can improve and develop more.

References

[1]. Amatyakul, P. *Two-dimensional joint inversion of Direct-current resistivity data and Magnetotelluric data*. Mahidol University, 2010.

[2]. Noisagool, S. *A Comparison between Stochastic and Deterministic optimization techniques using for Vertical Electrical Sounding (VES) inversion*. Mahidol University, 2014.

[3]. Ghosh, D. *Inverse filter coefficients for the computation of apparent resistivity standard curve for a horizontally stratified earth*. Geophysics prospecting, 2006.

[4]. Niculescu, B. *Forward Modelling of Vertical Soundings with Applications in the study of Sea Water Intrusions*. Section Applied and Environmental Geophysics. University of Buchaser, 2018.

[5]. Esben Aukan. *Piecewise 1D laterally constrained inversion of resistivity data*. Geophysical Prospecting, 2005.

[6]. U.S. Geological Survey. *MATLAB code for data-driven initial model of 1D Schlumberger sounding curve*. Geophysics, 2017

[7]. Dieter W. *A tool for designing digital filters for the Hankel and Fourier transforms in potential, diffusive, and wave field modeling*. Geophysics, 2019.

[8]. Ojo, A. O. and Olorunfemi, M. O. *A Graphical User Interface (GUI) MATLAB Program synthetic VES for computation of theoretical SCHLUMBERGER Vertical Electrical Sounding (VES) Curves for Multilayered earth models*. Ife Journal of Science, 2013.

[9]. Obiora D. *Geoelectrical evaluation of groundwater potentials of Bwari basement area, Central Nigeria*. International journal of physical sciences, 2013.

[10]. Kearey P. *An introduction to Geophysical exploration*. Blackwell Science Ltd, 2002.

[11]. Koeford O. *A semi-direct method of interpreting resistivity observations*. Geophysical Prospecting, 1965.

[12]. Vachiratienchai C. *Two-dimensional direct current resistivity inversion : finite difference method*. Mahidol University, 2007.

[13]. Boonchaisuk S. *Two-dimensional direct current resistivity inversion : finite element method*. Mahidol University, 2007.